

Continuum limit of a qubit-regularized SU(3) lattice gauge theory with glueballs

Rui Xian Siew ^{1,*}, Shailesh Chandrasekharan ^{1,†} and Tanmoy Bhattacharya ^{2,‡}

¹*Department of Physics, Box 90305, Duke University, Durham, North Carolina 27708, USA*

²*Theoretical Division, Los Alamos National Laboratory, Los Alamos, New Mexico 87545, USA*

(Dated: March 3, 2026)

We show that a simple qubit-regularized SU(3) lattice gauge theory (LGT) on a plaquette chain admits a continuum limit with massive glueball excitations, providing a minimal toy model of strong interactions without quarks. By mapping the plaquette-chain Hamiltonian to the three-state quantum clock model in a magnetic field, we demonstrate that the theory can be tuned to a continuum limit governed at short distances by the \mathbb{Z}_3 parafermion conformal field theory (CFT), which serves as the ultraviolet (UV) fixed point. A small relevant magnetic perturbation then drives the system to a massive continuum quantum field theory in the infrared (IR). The resulting relativistic massive particles can be interpreted as quasi one-dimensional analogues of glueballs. In the continuum theory we compute the ratio of the lowest glueball masses with opposite charge conjugation to be $m^-/m^+ = 1.459(2)$ and find $\sqrt{\sigma}/m^+ = 0.2648(2)$, where σ is the string tension between a static quark and antiquark.

Glueballs mediate the strong force between quarks, binding them into hadrons such as protons and neutrons. Unlike photons, glueballs also interact among themselves and, in the absence of quarks, can form massive bound states known as glueballs. Their dynamics are described by SU(3) Yang-Mills (YM) theory, a non-Abelian gauge theory in the continuum with eight gluons as fundamental degrees of freedom. Despite its conceptual simplicity, determining the glueball spectrum is notoriously difficult. The standard approach is to discretize the theory on a lattice, following Wilson, and compute the energy eigenvalues of the resulting Hamiltonian while taking the thermodynamic and continuum limits [1].

Recently, a new approach to SU(3) YM theory has aimed to reformulate it as an LGT with a finite-dimensional local Hilbert space. We refer to such constructions as qubit regularizations [2], since they can be encoded in qubits and potentially solved on a quantum computer [3]. Their viability relies on Wilsonian universality and renormalization [4]: the qubit-regularized theory must exhibit a relativistic quantum critical point whose long-distance physics is governed by the asymptotically free fixed point. With a relevant perturbation, this fixed point becomes the UV fixed point of the continuum theory, generating massive glueballs in the IR. Asymptotic freedom in such qubit-regularized theories may also emerge through more exotic renormalization group (RG) flows [5, 6].

Research on continuum limits of qubit-regularized LGTs is still in its infancy. If simple qubit-regularized SU(3) LGTs in 3+1 dimensions possess relativistic critical points, it is plausible that their long-distance physics would reproduce the asymptotically free fixed point of SU(3) YM theory, consistent with the expectation that only a few such fixed points exist in higher dimensions. Although qubit-regularized SU(3) LGTs in 3+1 dimensions are

difficult to study, they are more tractable in 1+1 dimensions, where RG fixed points are easier to find and identify. Even so, this direction remains relatively unexplored. If such continuum limits do exist, they could provide useful toy models of 3+1-dimensional SU(3) YM theory and potentially shed light on the dynamical origin of glueball masses.

In this work we demonstrate for the first time that a qubit-regularized SU(3) LGT admits a massive continuum limit. We introduce a concrete model on a plaquette chain, show how to approach this limit, and compute in that regime the ratio of two distinct nonperturbatively generated mass scales. The physical Hilbert space of the SU(3) plaquette chain is constructed in the monomer-dimer tensor-network (MDTN) basis [7], where gauge degrees of freedom reside on links connecting neighboring sites and are labeled by dimer tensor (equivalently, color-flux) states $|\lambda\rangle$ with $\lambda = \mathbf{1}, \mathbf{3}, \bar{\mathbf{3}}$, the irreducible representations of SU(3). A representative physical basis state is shown in Fig. 1.

The ladder geometry of the plaquette chain allows us to distinguish links along the chain and those along the rungs, which we denote by ℓ_c and ℓ_r , respectively. Elementary plaquettes P are defined as the squares formed by four such links. Owing to this geometry, the physical Hilbert space of the theory naturally splits into three topologically distinct sectors. The first sector, \mathcal{H}_I , consists of basis states in which the top and bottom chain links of every plaquette P are either $|\mathbf{1}, \mathbf{1}\rangle$, $|\mathbf{3}, \bar{\mathbf{3}}\rangle$, or $|\bar{\mathbf{3}}, \mathbf{3}\rangle$. The second sector, \mathcal{H}_{II} , contains plaquettes in the states $|\bar{\mathbf{3}}, \bar{\mathbf{3}}\rangle$, $|\mathbf{1}, \mathbf{3}\rangle$, or $|\mathbf{3}, \mathbf{1}\rangle$, while the third sector, \mathcal{H}_{III} , contains plaquettes in the states $|\mathbf{3}, \mathbf{3}\rangle$, $|\mathbf{1}, \bar{\mathbf{3}}\rangle$, or $|\bar{\mathbf{3}}, \mathbf{1}\rangle$. Under charge conjugation \hat{C} , $\mathbf{3}$ and $\bar{\mathbf{3}}$ are exchanged. Consequently, \mathcal{H}_I is invariant under charge conjugation, whereas the sectors \mathcal{H}_{II} and \mathcal{H}_{III} are exchanged into one another. Each of the latter sectors therefore breaks charge conjugation symmetry individually.

Plaquette chains have been used as a simplified class of quasi-one-dimensional lattice geometries to study LGTs especially on quantum computers [8–10]. Specializing to

* ruixian.siew@duke.edu

† sch27@duke.edu

‡ tanmoy@lanl.gov

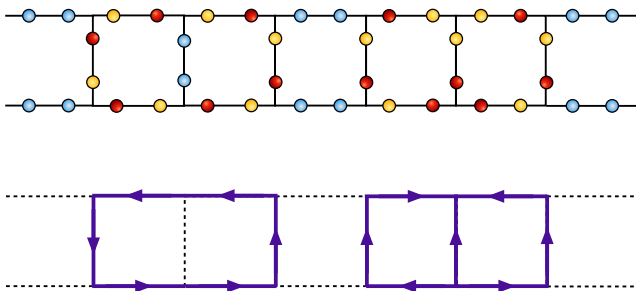


FIG. 1. Physical basis state of the qubit-regularized SU(3) LGT on a plaquette chain in the MDTN basis. Links are represented by dimer tensor states, which may equivalently be viewed as color flux states $|\lambda\rangle$, where $\lambda = \mathbf{1}$ (blue), $\mathbf{3}$ (red), and $\bar{\mathbf{3}}$ (yellow) are irreducible representations of SU(3). The two indices of each tensor are associated with the lattice sites connected by the link and transform in the irreps λ and its conjugate $\bar{\lambda}$. Gauge invariance enforces that the irreps meeting at each site combine to a singlet, implying for a plaquette chain the only possibilities are (i) a singlet, a triplet, and an anti-triplet index, (ii) three triplet indices, or (iii) three anti-triplet indices meeting at a site (top). An equivalent representation in terms of color fluxes is shown in the bottom panel, where a dashed line denotes the state $|\mathbf{1}\rangle$, arrows pointing to the right or upward denote $|\mathbf{3}\rangle$, and oppositely oriented arrows denote $|\bar{\mathbf{3}}\rangle$.

SU(3), the above simple Hilbert space has also been explored previously [11–13]. However, most earlier work focused on models based on the traditional Kogut–Susskind Hamiltonian with a single coupling [14], which cannot be tuned to a continuum limit. In Ref. [7] we proposed a class of simple gauge-invariant Hamiltonians for SU(N) LGTs that are free of sign problems. Adapting that construction to the SU(3) plaquette chain and introducing additional couplings, we propose the plaquette chain Hamiltonian,

$$H_{pc} = \kappa_c \sum_{\ell_c} \hat{\mathcal{E}}_{\ell_c} + \kappa_r \sum_{\ell_r} \hat{\mathcal{E}}_{\ell_r} - g \sum_P (\hat{U}_P + \hat{U}_P^\dagger), \quad (1)$$

where $\hat{\mathcal{E}}_\ell$ is diagonal in the link basis $|\lambda\rangle$ associated with link ℓ , with eigenvalue $(1 - \delta_{\lambda, \mathbf{1}})$. It assigns equal energies to the $\mathbf{3}$ and $\bar{\mathbf{3}}$ irreps, typically higher than that of the $\mathbf{1}$ irrep on each link, implying $\kappa_c, \kappa_r \geq 0$. In contrast, the plaquette operator \hat{U}_P and its Hermitian conjugate are off-diagonal in the MDTN basis and modify the irreps on the four links of a plaquette while preserving gauge invariance. Their action is illustrated in Fig. 2. To avoid sign problems in our Monte Carlo calculations, we restrict to $g \geq 0$. Finally, we note that $[H_{pc}, \hat{C}] = 0$, where \hat{C} is the charge-conjugation operator introduced earlier. Since the Hamiltonian is local and gauge invariant, it does not mix the three Hilbert spaces \mathcal{H}_I , \mathcal{H}_{II} , and \mathcal{H}_{III} . We identify \mathcal{H}_I as the vacuum sector. Introducing heavy static quarks and antiquarks at two sites generates a string of plaquettes connecting them that necessarily lies in one of the other two sectors. Thus, while the Hamiltonian retains the same form as in Eq. (1), the presence or absence of static charges alters the accessible Hilbert space and consequently affects

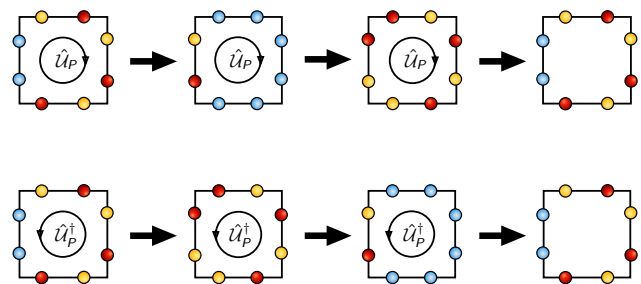


FIG. 2. Action of the plaquette operators \hat{U}_P and \hat{U}_P^\dagger on a representative MDTN state. Traversing the plaquette clockwise or counterclockwise updates the links according to the cyclic rule $\mathbf{1} \rightarrow \mathbf{3} \rightarrow \bar{\mathbf{3}} \rightarrow \mathbf{1}$, applied to the irrep at the first site of each link; the irrep at the opposite end is then fixed.

the energy spectrum.

Since the plaquettes admit only three quantum states within each Hilbert space sector, the SU(3) plaquette chain is equivalent, in each sector, to a one-dimensional three-state quantum clock model [13]. The latter is defined in terms of the operators

$$\hat{X} = \begin{pmatrix} 0 & 1 & 0 \\ 0 & 0 & 1 \\ 1 & 0 & 0 \end{pmatrix}, \quad \hat{Z} = \begin{pmatrix} 1 & 0 & 0 \\ 0 & e^{i2\pi/3} & 0 \\ 0 & 0 & e^{-i2\pi/3} \end{pmatrix}, \quad (2)$$

which act on the three states associated with each plaquette P . Restricting the Hamiltonian Eq. (1) to the sector \mathcal{H}_I yields

$$H_{\text{qcm}}^I = - \sum_P \left\{ J \hat{Z}_P \hat{Z}_{P+1}^\dagger + g \hat{X}_P + \frac{h}{3} \hat{Z}_P + \text{h.c.} \right\}, \quad (3)$$

with $J = \kappa_r/3$ and $h = 2\kappa_c$, up to an overall constant energy shift E_0 . In the remaining sectors \mathcal{H}_{II} and \mathcal{H}_{III} , the Hamiltonians H_{qcm}^{II} and H_{qcm}^{III} take the same form, except that h is replaced by $h = -\kappa_c$.

The quantum clock model defined in Eq. (3) is critical at $J = g = 1$ and $h = 0$, where its quantum critical behavior belongs to the universality class of the 2D three-state classical Potts model [15]. At this critical point, the infrared physics is described by a relativistic \mathbb{Z}_3 parafermion conformal field theory CFT with central charge $c = 4/5$ [16]. Via the mapping from Eq. (1) to Eq. (3), the same quantum critical point is realized in the qubit-regularized SU(3) plaquette chain at $\kappa_r = 3$, $g = 1$, and $\kappa_c = 0$, where we must identify the parafermions as the quasi-one-dimensional analogues of the gauge bosons¹. Relevant perturbations of the parafermion CFT, in the

¹ A strictly one-dimensional gauge theory has no local propagating degrees of freedom. Our model has rungs connecting two chains, and allows transverse, or ‘rung’-polarized, gauge bosons that are expected to be described as adjoint one-dimensional scalars. The parafermions in the UV presumably describe the physics of these bosons.

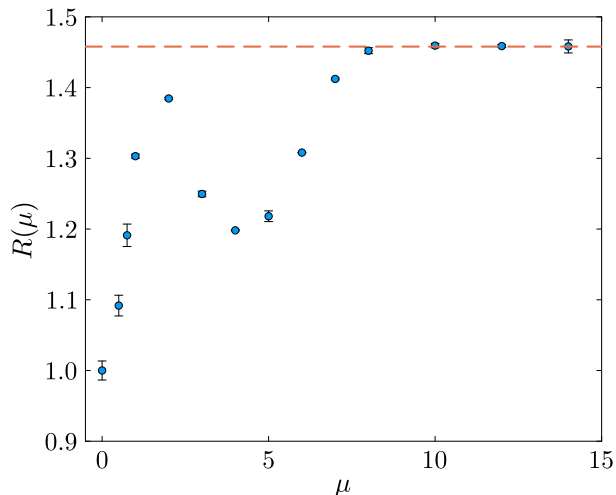


FIG. 3. Plot of the mass ratio $R(\mu)$ in Eq. (5) as a function of the scaling variable $\mu = h^{15/28}L$. The data points are obtained by extrapolating the DMRG data at each fixed value of μ to the joint limit $L \rightarrow \infty$ and $h \rightarrow 0$. The UV and IR regimes correspond to $\mu \rightarrow 0$ and $\mu \rightarrow \infty$, respectively. In the UV limit, the degeneracy of the lightest spin primaries related by charge conjugation at the \mathbb{Z}_3 parafermion CFT leads to the result that $R(0) = 1$ [17, 20]. In the IR limit, no closed-form expression for $R(\infty)$ is known since the theory is non-integrable.

form of a thermal coupling $\tau > 0$ with $\tau = g - 1$ and a magnetic coupling $h > 0$, generate massive quantum field theories [17]. In this work, we focus on the case $\tau = 0$ and $h > 0$ (equivalently, $\kappa_c > 0$), which arises naturally in the vacuum sector of the plaquette chain.

Since the correlation length associated with the magnetic perturbation diverges as $\xi \sim h^{-15/28}$ for $h \rightarrow 0$ [17–19], universal quantities in a finite system of L plaquettes arranged on a circle are functions of the dimensionless variable $\mu = h^{15/28}L$. One particularly interesting universal quantity is the mass ratio m^-/m^+ , where m^- and m^+ denote the masses of the lightest stable \hat{C} -odd and \hat{C} -even particles, respectively. These mass ratios can be extracted from the eigenvalues of Eq. (3) as a function of μ from the UV regime where $\mu \rightarrow 0$ to the IR regime where $\mu \rightarrow \infty$. We will be interested in the IR regime where the lattice model describes the massive quantum field theory (QFT), and the corresponding massive excitations may be viewed as quasi-one-dimensional analogues of glueballs.

In this work, we use DMRG to determine m^-/m^+ as a function of μ . We compute the low-energy spectrum of Eq. (3) at $J = g = 1$ for various values of μ . For each μ , we consider five lattice sizes $L = 32, 48, 64, 80$, and 96, which enables a controlled extrapolation to the thermodynamic limit. In each case, h is tuned to realize the desired value of μ . We denote the ground-state energy at fixed (L, μ) by $E_0^+(L, \mu)$, and the excited energies by $E_i^C(L, \mu)$, where $C = \pm$ labels the charge-conjugation eigenvalue and $i = 1, 2, \dots$ orders the states by increasing energy within each sector.

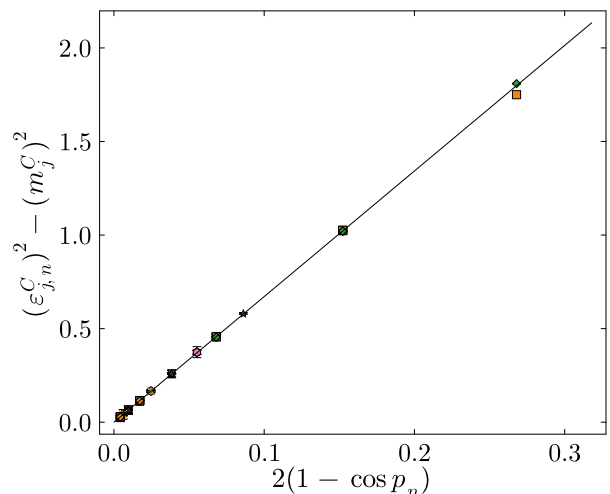


FIG. 4. Relativistic dispersion relation defined in Eq. (8). The straight line is a linear fit to all data points (87 in total) with $48 \leq L \leq 96$ and $10.0 \leq \mu \leq 14.0$. The slope yields ζ^2 , giving $\zeta = 2.5907(2)$ with $\chi^2/\text{d.o.f.} = 1.73$.

We extract the lowest glueball masses in the charge-conjugation-even and -odd sectors as

$$m^C(L, \mu) = E_1^C(L, \mu) - E_0^+(L, \mu). \quad (4)$$

To obtain the dimensionless ratio m^-/m^+ in the large- L limit, we assume that for sufficiently large L ,

$$\frac{m^-(L, \mu)}{m^+(L, \mu)} = R(\mu) - \frac{A(\mu)}{L}, \quad (5)$$

where $R(\mu)$ and $A(\mu)$ are μ -dependent coefficients. This ansatz provides a good fit at all values of μ [21]. The extracted $R(\mu)$ is shown in Fig. 3. We observe non-monotonic behavior at intermediate μ , while for $\mu \geq 8$ the ratio begins to saturate toward its IR value. Although we do not have a simple explanation for this non-monotonicity, similar behavior has been observed in traditional lattice calculations of glueball masses, where it is attributed to the presence of a critical point in the fundamental–adjoint coupling plane at which the scalar glueball mass vanishes [22]. The extracted coefficients in the large μ regime are listed in Table I, yielding the estimate

$$m^-/m^+ \approx 1.459(2). \quad (6)$$

This ratio was previously computed numerically using the truncated conformal space approach in Ref. [17], since the massive QFT emerging in the IR is non-integrable [23]. Because the earlier results were presented graphically, extracting a precise numerical value is difficult; however, a rough estimate indicates consistency with our result.

In order to confirm that the massive continuum QFT emerging in the IR is relativistic, we study the dispersion relation of the low-energy spectrum of Eq. (3). Since

μ	$A(\mu)$	$R(\mu)$	$\sqrt{\sigma}/m^+$
8.0	1.1(1)	1.452(4)	0.2676(4)
10.0	1.3(1)	1.459(3)	0.2649(2)
12.0	1.57(8)	1.459(2)	0.2648(2)
14.0	1.8(3)	1.458(9)	0.264(1)

TABLE I. The value of the ratio $R(\mu)$ and $A(\mu)$, obtained by extrapolating the data at $L = 32, 48, 64, 80, 96$ to the thermodynamic limit using the ansatz Eq. (5) at different values μ .

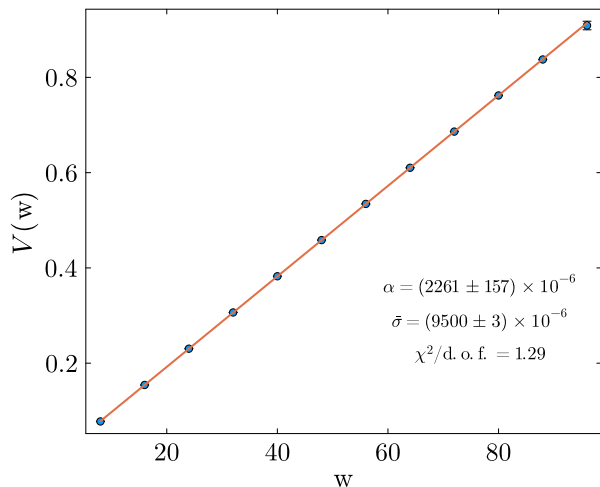


FIG. 5. Static quark potential $V(w)$ versus separation w for $L = 96$ and $\mu = 14.0$. The solid line is a linear fit whose slope gives $\bar{\sigma} = 0.009500(3)$.

the system is invariant under discrete translations, each energy eigenvalue $E_i^C(L, \mu)$ carries a definite lattice momentum $p_n = 2\pi n/L$. Single-particle excitations of different particles below the two-particle threshold can be identified as non-degenerate states at zero momentum. Using this insight, we reorganize the low-energy spectrum $E_i^C(L, \mu)$ by relabeling the index i as a pair (j, n) . We denote the vacuum energy $E_0^+(L, \mu)$ by $(j = 0, n = 0)$. The higher-energy states (in both sectors) correspond to the j -th massive particle with lattice momentum p_n . We denote the corresponding energies by $E_{j,n}^C(L, \mu)$ [21].

From these, we define the single-particle excitation energies by subtracting the vacuum energy,

$$\epsilon_{j,n}^C(L, \mu) = E_{j,n}^C(L, \mu) - E_0^+(L, \mu). \quad (7)$$

The mass of the j -th particle is then defined as $m_j^C = \epsilon_{j,0}^C(L, \mu)$. The dispersion relation

$$(\epsilon_{j,n}^C)^2 - (m_j^C)^2 = 2(1 - \cos p_n)\zeta^2 + \mathcal{O}(n^4 L^{-4}), \quad (8)$$

where ζ is a constant (independent of n , L , and j) that plays the role of $\hbar c$ converting inverse lattice spacing into energy units, is a hallmark of a relativistic particle.

As shown in Fig. 4, our data are well described by this dispersion relation, yielding $\zeta = 2.5907(2)$.

For sufficiently large L and μ , we can also compute the string tension between a static quark–antiquark pair by placing the quark at site $x = 0$ and the antiquark at $x = w$, both on the lower chain. Although the Hamiltonian remains that of Eq. (1), the Hilbert space is modified: the plaquettes between $x = 0$ and $x = w$ are forced into sector II, while the remaining plaquettes remain in the vacuum sector I. In the effective quantum clock model Eq. (3), this corresponds to a modification of the coupling h : on the plaquettes between $x = 0$ and $x = w$, h is reduced by a factor of two and changes sign relative to its value on the remaining plaquettes.

The heavy quark–antiquark potential is defined as

$$V(w) = E_0^+(w) - E_0^+, \quad (9)$$

where $E_0^+(w)$ denotes the ground-state energy in the presence of a static quark–antiquark pair separated by w , and E_0^+ is the vacuum ground-state energy. In the confined phase we expect a linear potential,

$$V(w) = \alpha + \bar{\sigma} w, \quad (10)$$

with $\bar{\sigma}$ the string tension (energy per unit length). In Fig. 5 we show an illustration of how we can extract $\bar{\sigma}$ from our data when $L = 96$ and $\mu = 14$.

Defining $\sigma = \bar{\sigma} \zeta$, which has dimensions of energy squared, and using the value of ζ extracted from the dispersion analysis, we compute the dimensionless ratio $\sqrt{\sigma}/m^+$ for each μ and L . Assuming the finite-size corrections are of the form L^{-1} , we extrapolate to the thermodynamic limit [21]. The resulting estimates of $\sqrt{\sigma}/m^+$ are listed in the fourth column of Table I, from which we obtain

$$\sqrt{\sigma}/m^+ = 0.2648(2).$$

Our work demonstrates that simple qubit-regularized SU(3) LGTs can exhibit nontrivial continuum limits with massive relativistic excitations analogous to glueballs. A similar massive continuum limit was recently identified in a qubit-regularized SU(2) theory [24]. Although both results arise in quasi-one-dimensional models, the underlying quantum critical points are related, from the gauge-theoretic perspective, to confinement–deconfinement transitions. For small nonzero h , the ground state of Eq. (3) lies in the ordered phase with $g/J < 1$, where h selects one of three degenerate vacua, corresponding to confinement. For $g/J > 1$, the ground state is disordered and largely insensitive to h , corresponding instead to deconfinement. It is plausible that analogous quantum critical points associated with confinement–deconfinement transitions exist in higher dimensions. Identifying such points in simple qubit-regularized SU(3) gauge theories and determining whether they give rise to massive continuum QFTs would be an important next step. In three spatial dimensions, such theories would presumably correspond either to conventional YM theory or to a more exotic variant enabled by qubit regularization.

ACKNOWLEDGMENTS

S.C. conceived of the idea and R.X.S carried out the investigations of this theory. Both of them created the outline of the manuscript. R.X.S. did all the DMRG calculations. The two together produced the first draft of the paper. T.B. checked the correctness of the physics discussed and provided further interpretation of the model in terms of a pseudo-one-dimensional gauge theory. All three authors refined the manuscript and agree with its final version.

We acknowledge the use of AI assistance, specifically

ChatGPT [25], in refining the language and clarity of this manuscript and providing citation to itself, before our final rounds of manual review and revision by all authors. S.C. and R.X.S. are supported in part by the U.S. Department of Energy, Office of Science, Nuclear Physics program under Award No. DE-FG02-05ER41368. T.B. was supported by the U.S. Department of Energy, Office of Science, Office of High Energy Physics under contract number KA2401012 (LANLE83G) at Los Alamos National Laboratory operated by Triad National Security, LLC, for the National Nuclear Security Administration of the U.S. Department of Energy (Contract No. 89233218CNA000001).

-
- [1] A. Athenodorou and M. Teper, The glueball spectrum of SU(3) gauge theory in 3 + 1 dimensions, *JHEP* **11** (11), 172, arXiv:2007.06422 [hep-lat].
- [2] S. Chandrasekharan, Qubit Regularization of Quantum Field Theories, *PoS LATTICE2024*, 001 (2025), arXiv:2502.05716 [hep-lat].
- [3] C. W. Bauer, Z. Davoudi, N. Klco, and M. J. Savage, Quantum simulation of fundamental particles and forces, *Nature Rev. Phys.* **5**, 420 (2023), arXiv:2404.06298 [hep-ph].
- [4] K. G. Wilson, The renormalization group and critical phenomena, *Rev. Mod. Phys.* **55**, 583 (1983).
- [5] T. Bhattacharya, A. J. Buser, S. Chandrasekharan, R. Gupta, and H. Singh, Qubit regularization of asymptotic freedom, *Phys. Rev. Lett.* **126**, 172001 (2021), arXiv:2012.02153 [hep-lat].
- [6] S. Maiti, D. Banerjee, S. Chandrasekharan, and M. K. Marinkovic, Asymptotic freedom at the Berezinskii-Kosterlitz-Thouless transition without fine-tuning using a qubit regularization, *Phys. Rev. Lett.* **132**, 041601 (2024), arXiv:2307.06117 [hep-lat].
- [7] S. Chandrasekharan, R. X. Siew, and T. Bhattacharya, Monomer-dimer tensor-network basis for qubit-regularized lattice gauge theories, *Phys. Rev. D* **111**, 114502 (2025), arXiv:2502.14175 [hep-lat].
- [8] S. Pradhan, A. Maroncelli, and E. Ercolessi, Discrete Abelian lattice gauge theories on a ladder and their dualities with quantum clock models, *Phys. Rev. B* **109**, 064410 (2024), arXiv:2208.04182 [hep-lat].
- [9] X. Yao, SU(2) gauge theory in 2 + 1 dimensions on a plaquette chain obeys the eigenstate thermalization hypothesis, *Phys. Rev. D* **108**, L031504 (2023), arXiv:2303.14264 [hep-lat].
- [10] L. Ebner, A. Schäfer, C. Seidl, B. Müller, and X. Yao, Entanglement entropy of (2+1)-dimensional SU(2) lattice gauge theory on plaquette chains, *Phys. Rev. D* **110**, 014505 (2024).
- [11] A. Ciavarella, N. Klco, and M. J. Savage, Trailhead for quantum simulation of SU(3) Yang-Mills lattice gauge theory in the local multiplet basis, *Phys. Rev. D* **103**, 094501 (2021).
- [12] S. V. Kadam, A. Naskar, I. Raychowdhury, and J. R. Stryker, Loop-string-hadron approach to SU(3) lattice Yang-Mills theory: Hilbert space of a trivalent vertex, *Phys. Rev. D* **111**, 074516 (2025).
- [13] V. Chen, B. Müller, and X. Yao, Minimally Truncated SU(3) Lattice Gauge Theory and String Tension, preprint archive (2026), arXiv:2601.10065 [hep-lat].
- [14] J. B. Kogut and L. Susskind, Hamiltonian formulation of Wilson's lattice gauge theories, *Phys. Rev. D* **11**, 395 (1975).
- [15] S. Elitzur, R. B. Pearson, and J. Shigemitsu, Phase structure of discrete Abelian spin and gauge systems, *Phys. Rev. D* **19**, 3698 (1979).
- [16] V. A. Fateev and A. B. Zamolodchikov, Parafermionic currents in the two-dimensional conformal quantum field theory and self-dual critical points in Z_N symmetric statistical systems, *Sov. Phys. JETP* **62**, 215 (1985).
- [17] L. Lepori, G. Z. Toth, and G. Delfino, Particle spectrum of the 3-state Potts field theory: A numerical study, *J. Stat. Mech.* **0911**, P11007 (2009), arXiv:0909.2192 [hep-th].
- [18] J. Cardy, *Scaling and renormalization in statistical physics*, Vol. 5 (Cambridge university press, 1996).
- [19] R. S. K. Mong, D. J. Clarke, J. Alicea, N. H. Lindner, and P. Fendley, Parafermionic conformal field theory on the lattice, *Journal of Physics A: Mathematical and Theoretical* **47**, 452001 (2014).
- [20] J. L. Cardy, Operator content of two-dimensional conformally invariant theories, *Nuclear Physics B* **270**, 186 (1986).
- [21] (2026), further details can be found in the Supplementary Materials enclosed with this paper.
- [22] U. M. Heller, SU(3) lattice gauge theory in the fundamental adjoint plane and scaling along the Wilson axis, *Phys. Lett. B* **362**, 123 (1995), arXiv:hep-lat/9508009.
- [23] V. Fateev, Integrable deformations in Z_N -symmetrical models of the conformal quantum field theory, *International Journal of Modern Physics A* **06**, 2109 (1991), <https://doi.org/10.1142/S0217751X91001052>.
- [24] R. X. Siew, S. Chandrasekharan, and T. Bhattacharya, Asymptotic-freedom and massive glueballs in a qubit-regularized SU(2) gauge theory, preprint (2025), arXiv:2512.11068 [hep-lat].
- [25] OpenAI, *Chatgpt (gpt-4)* (2025), accessed: 2025-02-14.

SUPPLEMENTARY MATERIAL

Continuum limit of a qubit-regularized SU(3) lattice gauge theory with glueballs

Rui Xian Siew, Shailesh Chandrasekharan, and Tanmoy Bhattacharya

A. Low energy spectrum in the vacuum sector

$L = 24, \mu = 0.0, C = +$				
i	E_i^+	δE_i^+	j	n
0	-5.850916e+01	7.87e-05	0	0
1	-5.841808e+01	7.48e-05	1	0
2	-5.773844e+01	8.34e-05	1	1
3	-5.773844e+01	8.46e-05	1	1

$L = 24, \mu = 0.0, C = -$				
i	E_i^-	δE_i^-	j	n
0	-5.841808e+01	7.53e-05	1	0
1	-5.773844e+01	7.49e-05	1	1
2	-5.773844e+01	8.43e-05	1	1
3	-5.760537e+01	1.05e-04	2	0

$L = 24, \mu = 0.5, C = +$				
i	E_i^+	δE_i^+	j	n
0	-5.850950e+01	7.63e-05	0	0
1	-5.842190e+01	7.48e-05	1	0
2	-5.774067e+01	8.45e-05	1	1
3	-5.774067e+01	7.56e-05	1	1

$L = 24, \mu = 0.5, C = -$				
i	E_i^-	δE_i^-	j	n
0	-5.841395e+01	7.57e-05	1	0
1	-5.773625e+01	8.16e-05	1	1
2	-5.773625e+01	7.72e-05	1	1
3	-5.760569e+01	1.05e-04	2	0

$L = 24, \mu = 0.75, C = +$				
i	E_i^+	δE_i^+	j	n
0	-5.851074e+01	7.61e-05	0	0
1	-5.842541e+01	7.73e-05	1	0
2	-5.774322e+01	8.41e-05	1	1
3	-5.774322e+01	7.99e-05	1	1

$L = 24, \mu = 0.75, C = -$				
i	E_i^-	δE_i^-	j	n
0	-5.840928e+01	7.50e-05	1	0
1	-5.773380e+01	7.51e-05	1	1
2	-5.773380e+01	8.47e-05	1	1
3	-5.760607e+01	1.05e-04	2	0

$L = 24, \mu = 1.0, C = +$				
i	E_i^+	δE_i^+	j	n
0	-5.851398e+01	7.48e-05	0	0
1	-5.842862e+01	7.65e-05	1	0
2	-5.774670e+01	8.33e-05	1	1
3	-5.774670e+01	8.17e-05	1	1

$L = 24, \mu = 1.0, C = -$				
i	E_i^-	δE_i^-	j	n
0	-5.840303e+01	7.63e-05	1	0
1	-5.773058e+01	8.33e-05	1	1
2	-5.773058e+01	7.69e-05	1	1
3	-5.707537e+01	2.46e-03	1	2

$L = 24, \mu = 2.0, C = +$				
i	E_i^+	δE_i^+	j	n
0	-5.856628e+01	7.62e-05	0	0
1	-5.841944e+01	7.66e-05	1	0
2	-5.777049e+01	7.50e-05	1	1
3	-5.777049e+01	8.23e-05	1	1

$L = 24, \mu = 2.0, C = -$				
i	E_i^-	δE_i^-	j	n
0	-5.836352e+01	7.73e-05	1	0
1	-5.771176e+01	7.97e-05	1	1
2	-5.771176e+01	8.53e-05	1	1
3	-5.709239e+01	2.72e-03	1	2

$L = 24, \mu = 3.0, C = +$				
i	E_i^+	δE_i^+	j	n
0	-5.868241e+01	7.31e-05	0	0
1	-5.837771e+01	7.69e-05	1	0
2	-5.781290e+01	7.56e-05	1	1
3	-5.781290e+01	7.82e-05	1	1

$L = 24, \mu = 3.0, C = -$				
i	E_i^-	δE_i^-	j	n
0	-5.830300e+01	7.51e-05	1	0
1	-5.768912e+01	3.04e-04	1	1
2	-5.768912e+01	2.51e-04	1	1
3	-5.712302e+01	2.03e-04	1	2

TABLE S1. Low energy spectrum of the quantum clock model at various values of $\mu = h^{15/28}L$ in the two charge-conjugation sectors at $L = 24$.

$L = 24, \mu = 4.0, C = +$				
i	E_i^+	δE_i^+	j	n
0	-5.885019e+01	7.31e-05	0	0
1	-5.832573e+01	7.55e-05	1	0
2	-5.787899e+01	7.63e-05	1	1
3	-5.787899e+01	7.54e-05	1	1

$L = 24, \mu = 4.0, C = -$				
i	E_i^-	δE_i^-	j	n
0	-5.822457e+01	7.74e-05	1	0
1	-5.767407e+01	4.82e-03	1	1
2	-5.767414e+01	1.57e-03	1	1
3	-5.717168e+01	6.85e-04	1	2

$L = 24, \mu = 7.0, C = +$				
i	E_i^+	δE_i^+	j	n
0	-5.964230e+01	7.15e-05	0	0
1	-5.845812e+01	7.67e-05	1	0
2	-5.827234e+01	7.55e-05	1	1
3	-5.827234e+01	7.53e-05	1	1

$L = 24, \mu = 7.0, C = -$				
i	E_i^-	δE_i^-	j	n
0	-5.800538e+01	7.49e-05	1	0
1	-5.782229e+01	7.94e-05	1	1
2	-5.782229e+01	7.44e-05	1	1
3	-5.724916e+01	1.88e-04	1	2

$L = 24, \mu = 8.0, C = +$				
i	E_i^+	δE_i^+	j	n
0	-6.000141e+01	7.42e-05	0	0
1	-5.864163e+01	7.41e-05	1	0
2	-5.848177e+01	7.56e-05	1	1
3	-5.848177e+01	7.52e-05	1	1

$L = 24, \mu = 8.0, C = -$				
i	E_i^-	δE_i^-	j	n
0	-5.808616e+01	7.67e-05	1	0
1	-5.796069e+01	7.60e-05	1	1
2	-5.796069e+01	7.55e-05	1	1
3	-5.765286e+01	3.86e-04	1	2

$L = 24, \mu = 10.0, C = +$				
i	E_i^+	δE_i^+	j	n
0	-6.086137e+01	3.14e-04	0	0
1	-5.915841e+01	7.50e-05	1	0
2	-5.903077e+01	7.58e-05	1	1
3	-5.903077e+01	7.63e-05	1	1

$L = 24, \mu = 10.0, C = -$				
i	E_i^-	δE_i^-	j	n
0	-5.846969e+01	7.65e-05	1	0
1	-5.837711e+01	7.63e-05	1	1
2	-5.837711e+01	7.47e-05	1	1
3	-5.812171e+01	7.58e-05	1	2

$L = 24, \mu = 12.0, C = +$				
i	E_i^+	δE_i^+	j	n
0	-6.190946e+01	4.63e-04	0	0
1	-5.986487e+01	7.61e-05	1	0
2	-5.975859e+01	7.58e-05	1	1
3	-5.975859e+01	7.63e-05	1	1
4	-5.947145e+01	7.56e-05	1	2
5	-5.947145e+01	7.72e-05	1	2
6	-5.906790e+01	7.43e-05	1	3
7	-5.906790e+01	7.47e-05	1	3

$L = 24, \mu = 12.0, C = -$				
i	E_i^-	δE_i^-	j	n
0	-5.905819e+01	2.00e-04	1	0
1	-5.898151e+01	1.09e-04	1	1
2	-5.898151e+01	8.82e-05	1	1
3	-5.876468e+01	8.54e-05	1	2
4	-5.876468e+01	7.74e-05	1	2
5	-5.843921e+01	7.43e-05	1	3
6	-5.843921e+01	7.79e-05	1	3
7	-5.803885e+01	1.83e-03	1	4

$L = 24, \mu = 14.0, C = +$				
i	E_i^+	δE_i^+	j	n
0	-6.314472e+01	5.75e-04	0	0
1	-6.075872e+01	1.26e-04	1	0
2	-6.066815e+01	7.64e-05	1	1
3	-6.066815e+01	1.04e-04	1	1
4	-6.041801e+01	7.95e-05	1	2
5	-6.041801e+01	8.31e-05	1	2
6	-6.005622e+01	7.73e-05	1	3
7	-6.005622e+01	7.74e-05	1	3

$L = 24, \mu = 14.0, C = -$				
i	E_i^-	δE_i^-	j	n
0	-5.984086e+01	8.47e-04	1	0
1	-5.977547e+01	2.80e-04	1	1
2	-5.977547e+01	3.85e-04	1	1
3	-5.958829e+01	1.40e-04	1	2
4	-5.958829e+01	1.92e-04	1	2
5	-5.930195e+01	1.02e-04	1	3
6	-5.930195e+01	9.17e-05	1	3
7	-5.894418e+01	7.69e-05	1	4

TABLE S2. Low energy spectrum of the quantum clock model at various values of $\mu = h^{15/28}L$ in the two charge-conjugation sectors at $L = 24$.

$L = 32, \mu = 0.0, C = +$				
i	E_i^+	δE_i^+	j	n
0	-7.798574e+01	1.23e-04	0	0
1	-7.791749e+01	1.11e-04	1	0
2	-7.740734e+01	2.80e-04	1	1
3	-7.740734e+01	2.24e-04	1	1

$L = 32, \mu = 0.0, C = -$				
i	E_i^-	δE_i^-	j	n
0	-7.791749e+01	9.06e-05	1	0
1	-7.740734e+01	2.55e-04	1	1
2	-7.740734e+01	2.38e-04	1	1
3	-7.730700e+01	3.90e-04	2	0

$L = 32, \mu = 0.5, C = +$				
i	E_i^+	δE_i^+	j	n
0	-7.798599e+01	1.22e-04	0	0
1	-7.792037e+01	1.12e-04	1	0
2	-7.740901e+01	2.78e-04	1	1
3	-7.740901e+01	2.13e-04	1	1

$L = 32, \mu = 0.5, C = -$				
i	E_i^-	δE_i^-	j	n
0	-7.791439e+01	9.10e-05	1	0
1	-7.740569e+01	2.36e-04	1	1
2	-7.740569e+01	2.59e-04	1	1
3	-7.708089e+01	5.60e-04	1	2

$L = 32, \mu = 0.75, C = +$				
i	E_i^+	δE_i^+	j	n
0	-7.798693e+01	1.20e-04	0	0
1	-7.792300e+01	1.16e-04	1	0
2	-7.741093e+01	2.69e-04	1	1
3	-7.741093e+01	2.50e-04	1	1

$L = 32, \mu = 0.75, C = -$				
i	E_i^-	δE_i^-	j	n
0	-7.791088e+01	9.10e-05	1	0
1	-7.740385e+01	2.05e-04	1	1
2	-7.740385e+01	2.79e-04	1	1
3	-7.708089e+01	5.80e-04	1	2

$L = 32, \mu = 1.0, C = +$				
i	E_i^+	δE_i^+	j	n
0	-7.798935e+01	1.17e-04	0	0
1	-7.792541e+01	1.18e-04	1	0
2	-7.741354e+01	2.75e-04	1	1
3	-7.741354e+01	2.14e-04	1	1

$L = 32, \mu = 1.0, C = -$				
i	E_i^-	δE_i^-	j	n
0	-7.790619e+01	9.15e-05	1	0
1	-7.740143e+01	2.59e-04	1	1
2	-7.740143e+01	2.47e-04	1	1
3	-7.690542e+01	1.26e-02	1	2

$L = 32, \mu = 2.0, C = +$				
i	E_i^+	δE_i^+	j	n
0	-7.802863e+01	9.01e-05	0	0
1	-7.791855e+01	1.18e-04	1	0
2	-7.743143e+01	2.06e-04	1	1
3	-7.743143e+01	2.58e-04	1	1

$L = 32, \mu = 2.0, C = -$				
i	E_i^-	δE_i^-	j	n
0	-7.787651e+01	9.05e-05	1	0
1	-7.738724e+01	2.92e-04	1	1
2	-7.738724e+01	2.32e-04	1	1
3	-7.691892e+01	2.05e-02	1	2

$L = 32, \mu = 3.0, C = +$				
i	E_i^+	δE_i^+	j	n
0	-7.811585e+01	8.66e-05	0	0
1	-7.788732e+01	1.22e-04	1	0
2	-7.746336e+01	2.21e-04	1	1
3	-7.746336e+01	2.09e-04	1	1

$L = 32, \mu = 3.0, C = -$				
i	E_i^-	δE_i^-	j	n
0	-7.783103e+01	9.31e-05	1	0
1	-7.736999e+01	3.06e-04	1	1
2	-7.736998e+01	2.70e-03	1	1
3	-7.694256e+01	8.07e-04	1	2

$L = 32, \mu = 4.0, C = +$				
i	E_i^+	δE_i^+	j	n
0	-7.824189e+01	8.45e-05	0	0
1	-7.784850e+01	1.37e-04	1	0
2	-7.751316e+01	2.02e-04	1	1
3	-7.751316e+01	1.52e-04	1	1

$L = 32, \mu = 4.0, C = -$				
i	E_i^-	δE_i^-	j	n
0	-7.777206e+01	9.95e-05	1	0
1	-7.735808e+01	4.53e-04	1	1
2	-7.735807e+01	2.07e-03	1	1
3	-7.697850e+01	7.03e-04	1	2

$L = 32, \mu = 5.0, C = +$				
i	E_i^+	δE_i^+	j	n
0	-7.840443e+01	8.44e-05	0	0
1	-7.782533e+01	1.54e-04	1	0
2	-7.758505e+01	9.46e-04	1	1
3	-7.758505e+01	2.00e-04	1	1

$L = 32, \mu = 5.0, C = -$				
i	E_i^-	δE_i^-	j	n
0	-7.770339e+01	1.16e-04	1	0
1	-7.736346e+01	6.83e-04	1	1
2	-7.736220e+01	2.01e-03	1	1
3	-7.703176e+01	6.07e-04	1	2

$L = 32, \mu = 6.0, C = +$				
i	E_i^+	δE_i^+	j	n
0	-7.860298e+01	8.60e-05	0	0
1	-7.785674e+01	1.39e-04	1	0
2	-7.768288e+01	6.85e-04	1	1
3	-7.768288e+01	1.24e-04	1	1

$L = 32, \mu = 6.0, C = -$				
i	E_i^-	δE_i^-	j	n
0	-7.763505e+01	1.53e-04	1	0
1	-7.739713e+01	1.74e-03	1	1
2	-7.739688e+01	1.20e-03	1	1
3	-7.704389e+01	2.80e-03	1	2

TABLE S3. Low energy spectrum of the quantum clock model at various values of $\mu = h^{15/28}L$ in the two charge-conjugation sectors at $L = 32$.

$L = 32, \mu = 7.0, C = +$				
i	E_i^+	δE_i^+	j	n
0	-7.883735e+01	8.54e-05	0	0
1	-7.794991e+01	1.11e-04	1	0
2	-7.780968e+01	1.13e-04	1	1
3	-7.780968e+01	8.98e-05	1	1

$L = 32, \mu = 7.0, C = -$				
i	E_i^-	δE_i^-	j	n
0	-7.760402e+01	1.99e-04	1	0
1	-7.746474e+01	2.62e-04	1	1
2	-7.746474e+01	2.04e-04	1	1
3	-7.703667e+01	8.02e-04	1	2

$L = 32, \mu = 8.0, C = +$				
i	E_i^+	δE_i^+	j	n
0	-7.910746e+01	1.03e-04	0	0
1	-7.808847e+01	9.34e-05	1	0
2	-7.796758e+01	8.98e-05	1	1
3	-7.796758e+01	9.33e-05	1	1

$L = 32, \mu = 8.0, C = -$				
i	E_i^-	δE_i^-	j	n
0	-7.766163e+01	1.76e-04	1	0
1	-7.756689e+01	2.03e-04	1	1
2	-7.756689e+01	1.80e-04	1	1
3	-7.733444e+01	3.12e-04	1	2

$L = 32, \mu = 10.0, C = +$				
i	E_i^+	δE_i^+	j	n
0	-7.975458e+01	1.11e-04	0	0
1	-7.847839e+01	8.84e-05	1	0
2	-7.838149e+01	8.98e-05	1	1
3	-7.838149e+01	9.01e-05	1	1

$L = 32, \mu = 10.0, C = -$				
i	E_i^-	δE_i^-	j	n
0	-7.794557e+01	1.71e-04	1	0
1	-7.787576e+01	1.14e-04	1	1
2	-7.787576e+01	1.34e-04	1	1
3	-7.768242e+01	1.56e-04	1	2

$L = 32, \mu = 12.0, C = +$				
i	E_i^+	δE_i^+	j	n
0	-8.054374e+01	6.41e-04	0	0
1	-7.901139e+01	9.12e-05	1	0
2	-7.893035e+01	9.26e-05	1	1
3	-7.893035e+01	9.21e-05	1	1
4	-7.871034e+01	9.04e-05	1	2
5	-7.871034e+01	8.99e-05	1	2
6	-7.839795e+01	9.20e-05	1	3
7	-7.839795e+01	9.17e-05	1	3

$L = 32, \mu = 12.0, C = -$				
i	E_i^-	δE_i^-	j	n
0	-7.838342e+01	8.79e-05	1	0
1	-7.832538e+01	9.23e-05	1	1
2	-7.832538e+01	8.97e-05	1	1
3	-7.816059e+01	9.71e-05	1	2
4	-7.816059e+01	9.69e-05	1	2
5	-7.791121e+01	1.06e-04	1	3
6	-7.791121e+01	1.04e-04	1	3
7	-7.761681e+01	2.65e-03	1	4

$L = 32, \mu = 14.0, C = +$				
i	E_i^+	δE_i^+	j	n
0	-8.147438e+01	1.30e-03	0	0
1	-7.968590e+01	8.14e-04	1	0
2	-7.961647e+01	5.57e-04	1	1
3	-7.961647e+01	1.21e-04	1	1
4	-7.942376e+01	1.74e-04	1	2
5	-7.942376e+01	1.60e-04	1	2
6	-7.914210e+01	1.08e-04	1	3
7	-7.914210e+01	1.04e-04	1	3

$L = 32, \mu = 14.0, C = -$				
i	E_i^-	δE_i^-	j	n
0	-7.896675e+01	3.71e-04	1	0
1	-7.891701e+01	2.13e-04	1	1
2	-7.891701e+01	1.69e-04	1	1
3	-7.877402e+01	1.42e-04	1	2
4	-7.877402e+01	1.43e-04	1	2
5	-7.855342e+01	9.87e-05	1	3
6	-7.855342e+01	9.23e-05	1	3
7	-7.827426e+01	1.93e-04	1	4

$L = 48, \mu = 0.0, C = +$				
i	E_i^+	δE_i^+	j	n
0	-1.169503e+02	5.94e-04	0	0
1	-1.169048e+02	4.96e-04	1	0
2	-1.165645e+02	1.32e-03	1	1
3	-1.166746e+02	1.48e-03	2	0

$L = 48, \mu = 0.0, C = -$				
i	E_i^-	δE_i^-	j	n
0	-1.169048e+02	2.84e-04	1	0
1	-1.165645e+02	1.07e-03	1	1
2	-1.165645e+02	1.26e-03	1	1
3	-1.164973e+02	1.86e-03	2	0

TABLE S4. Low energy spectrum of the quantum clock model at various values of $\mu = h^{15/28}L$ in the two charge-conjugation sectors at $L = 32$.

$L = 48, \mu = 0.5, C = +$				
i	E_i^+	δE_i^+	j	n
0	-1.169504e+02	5.93e-04	0	0
1	-1.169067e+02	5.15e-04	1	0
2	-1.165657e+02	1.30e-03	1	1
3	-1.165657e+02	1.06e-03	1	1

$L = 48, \mu = 0.5, C = -$				
i	E_i^-	δE_i^-	j	n
0	-1.169027e+02	2.86e-04	1	0
1	-1.165634e+02	1.02e-03	1	1
2	-1.165634e+02	1.30e-03	1	1
3	-1.162260e+02	7.72e-03	1	2

$L = 48, \mu = 0.75, C = +$				
i	E_i^+	δE_i^+	j	n
0	-1.169510e+02	5.78e-04	0	0
1	-1.169085e+02	5.58e-04	1	0
2	-1.165669e+02	1.23e-03	1	1
3	-1.165669e+02	1.19e-03	1	1

$L = 48, \mu = 0.75, C = -$				
i	E_i^-	δE_i^-	j	n
0	-1.169004e+02	2.84e-04	1	0
1	-1.165622e+02	1.30e-03	1	1
2	-1.165622e+02	1.04e-03	1	1
3	-1.164975e+02	1.85e-03	2	0

$L = 48, \mu = 1.0, C = +$				
i	E_i^+	δE_i^+	j	n
0	-1.169527e+02	5.62e-04	0	0
1	-1.169101e+02	5.65e-04	1	0
2	-1.165687e+02	1.10e-03	1	1
3	-1.165687e+02	1.27e-03	1	1

$L = 48, \mu = 1.0, C = -$				
i	E_i^-	δE_i^-	j	n
0	-1.168973e+02	2.91e-04	1	0
1	-1.165606e+02	1.30e-03	1	1
2	-1.165606e+02	1.08e-03	1	1
3	-1.162259e+02	1.85e-02	1	2

$L = 48, \mu = 2.0, C = +$				
i	E_i^+	δE_i^+	j	n
0	-1.169789e+02	3.36e-04	0	0
1	-1.169055e+02	5.57e-04	1	0
2	-1.165806e+02	1.21e-03	1	1
3	-1.165806e+02	9.61e-04	1	1

$L = 48, \mu = 2.0, C = -$				
i	E_i^-	δE_i^-	j	n
0	-1.168774e+02	3.12e-04	1	0
1	-1.165511e+02	1.22e-03	1	1
2	-1.165511e+02	1.32e-03	1	1
3	-1.164995e+02	1.85e-03	2	0

$L = 48, \mu = 3.0, C = +$				
i	E_i^+	δE_i^+	j	n
0	-1.170371e+02	1.86e-04	0	0
1	-1.168848e+02	5.80e-04	1	0
2	-1.166020e+02	9.27e-04	1	1
3	-1.166020e+02	1.06e-03	1	1

$L = 48, \mu = 3.0, C = -$				
i	E_i^-	δE_i^-	j	n
0	-1.168470e+02	3.51e-04	1	0
1	-1.165394e+02	1.51e-03	1	1
2	-1.165394e+02	2.49e-03	1	1
3	-1.162528e+02	4.28e-03	1	2

$L = 48, \mu = 4.0, C = +$				
i	E_i^+	δE_i^+	j	n
0	-1.171213e+02	1.21e-04	0	0
1	-1.168590e+02	6.77e-04	1	0
2	-1.166354e+02	8.23e-04	1	1
3	-1.166354e+02	9.01e-04	1	1

$L = 48, \mu = 4.0, C = -$				
i	E_i^-	δE_i^-	j	n
0	-1.168076e+02	3.99e-04	1	0
1	-1.165309e+02	4.85e-03	1	1
2	-1.165310e+02	1.24e-03	1	1
3	-1.162765e+02	3.10e-03	1	2

$L = 48, \mu = 5.0, C = +$				
i	E_i^+	δE_i^+	j	n
0	-1.172299e+02	1.07e-04	0	0
1	-1.168439e+02	7.54e-04	1	0
2	-1.166836e+02	8.06e-04	1	1
3	-1.166836e+02	5.99e-04	1	1

$L = 48, \mu = 5.0, C = -$				
i	E_i^-	δE_i^-	j	n
0	-1.167617e+02	5.43e-04	1	0
1	-1.165336e+02	3.27e-03	1	1
2	-1.165338e+02	1.61e-03	1	1
3	-1.165321e+02	2.59e-03	2	0

$L = 48, \mu = 6.0, C = +$				
i	E_i^+	δE_i^+	j	n
0	-1.173626e+02	1.06e-04	0	0
1	-1.168655e+02	6.75e-04	1	0
2	-1.167492e+02	6.32e-04	1	1
3	-1.167492e+02	5.03e-04	1	1

$L = 48, \mu = 6.0, C = -$				
i	E_i^-	δE_i^-	j	n
0	-1.167156e+02	7.27e-04	1	0
1	-1.165550e+02	2.35e-03	1	1
2	-1.165549e+02	1.82e-03	1	1
3	-1.165551e+02	1.81e-03	2	0

$L = 48, \mu = 7.0, C = +$				
i	E_i^+	δE_i^+	j	n
0	-1.175193e+02	1.11e-04	0	0
1	-1.169282e+02	5.06e-04	1	0
2	-1.168343e+02	5.08e-04	1	1
3	-1.168343e+02	3.62e-04	1	1

$L = 48, \mu = 7.0, C = -$				
i	E_i^-	δE_i^-	j	n
0	-1.166932e+02	9.90e-04	1	0
1	-1.165991e+02	1.02e-03	1	1
2	-1.165991e+02	1.29e-03	1	1
3	-1.163153e+02	3.44e-03	1	2

TABLE S5. Low energy spectrum of the quantum clock model at various values of $\mu = h^{15/28}L$ in the two charge-conjugation sectors at $L = 48$.

$L = 48, \mu = 8.0, C = +$				
i	E_i^+	δE_i^+	j	n
0	-1.176999e+02	1.17e-04	0	0
1	-1.170213e+02	3.67e-04	1	0
2	-1.169402e+02	3.85e-04	1	1
3	-1.169402e+02	2.68e-04	1	1

$L = 48, \mu = 8.0, C = -$				
i	E_i^-	δE_i^-	j	n
0	-1.167296e+02	8.97e-04	1	0
1	-1.166661e+02	9.83e-04	1	1
2	-1.166661e+02	9.52e-04	1	1
3	-1.165107e+02	1.44e-03	1	2

$L = 48, \mu = 10.0, C = +$				
i	E_i^+	δE_i^+	j	n
0	-1.181329e+02	1.46e-04	0	0
1	-1.172831e+02	2.20e-04	1	0
2	-1.172179e+02	2.13e-04	1	1
3	-1.172179e+02	1.67e-04	1	1

$L = 48, \mu = 10.0, C = -$				
i	E_i^-	δE_i^-	j	n
0	-1.169165e+02	9.40e-04	1	0
1	-1.168699e+02	5.36e-04	1	1
2	-1.168699e+02	7.61e-04	1	1
3	-1.167404e+02	8.35e-04	1	2

$L = 48, \mu = 12.0, C = +$				
i	E_i^+	δE_i^+	j	n
0	-1.186612e+02	1.08e-04	0	0
1	-1.176408e+02	1.35e-04	1	0
2	-1.175861e+02	1.27e-04	1	1
3	-1.175861e+02	1.22e-04	1	1
4	-1.174371e+02	1.51e-04	1	2
5	-1.174371e+02	1.63e-04	1	2
6	-1.172242e+02	1.66e-04	1	3
7	-1.172242e+02	1.71e-04	1	3

$L = 48, \mu = 12.0, C = -$				
i	E_i^-	δE_i^-	j	n
0	-1.172062e+02	5.92e-04	1	0
1	-1.171674e+02	6.17e-04	1	1
2	-1.171674e+02	3.69e-04	1	1
3	-1.170568e+02	4.66e-04	1	2
4	-1.170568e+02	5.64e-04	1	2
5	-1.168885e+02	6.00e-04	1	3
6	-1.168885e+02	6.18e-04	1	3
7	-1.166947e+02	2.41e-03	1	4

$L = 48, \mu = 14.0, C = +$				
i	E_i^+	δE_i^+	j	n
0	-1.192846e+02	3.26e-03	0	0
1	-1.180936e+02	2.74e-04	1	0
2	-1.180466e+02	1.64e-04	1	1
3	-1.180466e+02	2.66e-04	1	1
4	-1.179156e+02	1.74e-04	1	2
5	-1.179156e+02	1.34e-04	1	2
6	-1.177228e+02	1.34e-04	1	3
7	-1.177228e+02	1.36e-04	1	3

$L = 48, \mu = 14.0, C = -$				
i	E_i^-	δE_i^-	j	n
0	-1.175929e+02	3.33e-03	1	0
1	-1.175595e+02	2.33e-03	1	1
2	-1.175595e+02	5.65e-04	1	1
3	-1.174633e+02	2.62e-04	1	2
4	-1.174633e+02	9.86e-04	1	2
5	-1.173139e+02	3.41e-04	1	3
6	-1.173139e+02	3.85e-04	1	3
7	-1.171233e+02	5.23e-04	1	4

$L = 64, \mu = 0.0, C = +$				
i	E_i^+	δE_i^+	j	n
0	-1.559204e+02	1.57e-03	0	0
1	-1.558864e+02	1.35e-03	1	0
2	-1.556312e+02	2.57e-03	1	1
3	-1.557142e+02	3.60e-03	2	0

$L = 64, \mu = 0.0, C = -$				
i	E_i^-	δE_i^-	j	n
0	-1.558864e+02	7.38e-04	1	0
1	-1.556312e+02	2.65e-03	1	1
2	-1.556312e+02	3.02e-03	1	1
3	-1.555806e+02	4.44e-03	2	0

$L = 64, \mu = 0.5, C = +$				
i	E_i^+	δE_i^+	j	n
0	-1.559206e+02	1.56e-03	0	0
1	-1.558878e+02	1.37e-03	1	0
2	-1.556320e+02	2.99e-03	1	1
3	-1.556320e+02	2.83e-03	1	1

$L = 64, \mu = 0.5, C = -$				
i	E_i^-	δE_i^-	j	n
0	-1.558848e+02	7.43e-04	1	0
1	-1.556303e+02	2.47e-03	1	1
2	-1.556303e+02	3.14e-03	1	1
3	-1.555806e+02	4.44e-03	2	0

TABLE S6. Low energy spectrum of the quantum clock model at various values of $\mu = h^{15/28}L$ in the two charge-conjugation sectors at $L = 48$.

$L = 64, \mu = 0.75, C = +$				
i	E_i^+	δE_i^+	j	n
0	-1.559210e+02	1.52e-03	0	0
1	-1.558891e+02	1.46e-03	1	0
2	-1.556330e+02	3.15e-03	1	1
3	-1.556330e+02	2.51e-03	1	1

$L = 64, \mu = 0.75, C = -$				
i	E_i^-	δE_i^-	j	n
0	-1.558831e+02	7.48e-04	1	0
1	-1.556294e+02	3.15e-03	1	1
2	-1.556294e+02	2.46e-03	1	1
3	-1.555807e+02	4.42e-03	2	0

$L = 64, \mu = 1.0, C = +$				
i	E_i^+	δE_i^+	j	n
0	-1.559222e+02	1.46e-03	0	0
1	-1.558903e+02	1.46e-03	1	0
2	-1.556343e+02	2.94e-03	1	1
3	-1.556343e+02	2.78e-03	1	1

$L = 64, \mu = 1.0, C = -$				
i	E_i^-	δE_i^-	j	n
0	-1.558807e+02	7.57e-04	1	0
1	-1.556282e+02	2.57e-03	1	1
2	-1.556282e+02	3.21e-03	1	1
3	-1.555808e+02	4.44e-03	2	0

$L = 64, \mu = 2.0, C = +$				
i	E_i^+	δE_i^+	j	n
0	-1.559419e+02	8.83e-04	0	0
1	-1.558869e+02	1.43e-03	1	0
2	-1.556433e+02	2.78e-03	1	1
3	-1.556433e+02	2.58e-03	1	1

$L = 64, \mu = 2.0, C = -$				
i	E_i^-	δE_i^-	j	n
0	-1.558658e+02	8.11e-04	1	0
1	-1.556210e+02	2.96e-03	1	1
2	-1.556210e+02	3.17e-03	1	1
3	-1.555821e+02	4.43e-03	2	0

$L = 64, \mu = 3.0, C = +$				
i	E_i^+	δE_i^+	j	n
0	-1.559856e+02	4.75e-04	0	0
1	-1.558714e+02	1.50e-03	1	0
2	-1.556593e+02	2.08e-03	1	1
3	-1.556593e+02	2.66e-03	1	1

$L = 64, \mu = 3.0, C = -$				
i	E_i^-	δE_i^-	j	n
0	-1.558430e+02	9.55e-04	1	0
1	-1.556122e+02	3.56e-03	1	1
2	-1.556122e+02	2.90e-03	1	1
3	-1.555856e+02	4.40e-03	2	0

$L = 64, \mu = 4.0, C = +$				
i	E_i^+	δE_i^+	j	n
0	-1.560488e+02	2.71e-04	0	0
1	-1.558521e+02	1.72e-03	1	0
2	-1.556844e+02	2.04e-03	1	1
3	-1.556844e+02	2.18e-03	1	1

$L = 64, \mu = 4.0, C = -$				
i	E_i^-	δE_i^-	j	n
0	-1.558134e+02	1.06e-03	1	0
1	-1.556057e+02	3.60e-03	1	1
2	-1.556055e+02	1.40e-02	1	1
3	-1.555933e+02	7.88e-03	2	0

$L = 64, \mu = 5.0, C = +$				
i	E_i^+	δE_i^+	j	n
0	-1.561304e+02	1.71e-04	0	0
1	-1.558409e+02	2.06e-03	1	0

$L = 64, \mu = 5.0, C = -$				
i	E_i^-	δE_i^-	j	n
0	-1.557788e+02	1.44e-03	1	0
1	-1.556072e+02	6.62e-03	1	1

$L = 64, \mu = 6.0, C = +$				
i	E_i^+	δE_i^+	j	n
0	-1.562300e+02	1.28e-04	0	0
1	-1.558574e+02	1.72e-03	1	0
2	-1.557701e+02	1.47e-03	1	1
3	-1.557701e+02	1.42e-03	1	1

$L = 64, \mu = 6.0, C = -$				
i	E_i^-	δE_i^-	j	n
0	-1.557441e+02	1.86e-03	1	0
1	-1.556231e+02	3.97e-03	1	1
2	-1.556229e+02	3.51e-03	1	1
3	-1.556229e+02	3.59e-03	2	0

$L = 64, \mu = 7.0, C = +$				
i	E_i^+	δE_i^+	j	n
0	-1.563477e+02	1.22e-04	0	0
1	-1.559047e+02	1.32e-03	1	0

$L = 64, \mu = 7.0, C = -$				
i	E_i^-	δE_i^-	j	n
0	-1.557266e+02	2.52e-03	1	0
1	-1.556557e+02	3.04e-03	1	1

$L = 64, \mu = 8.0, C = +$				
i	E_i^+	δE_i^+	j	n
0	-1.564834e+02	1.34e-04	0	0
1	-1.559748e+02	9.94e-04	1	0
2	-1.559138e+02	9.34e-04	1	1
3	-1.559138e+02	8.39e-04	1	1

$L = 64, \mu = 8.0, C = -$				
i	E_i^-	δE_i^-	j	n
0	-1.557532e+02	2.29e-03	1	0
1	-1.557055e+02	2.63e-03	1	1
2	-1.557055e+02	2.07e-03	1	1
3	-1.555889e+02	3.58e-03	1	2

TABLE S7. Low energy spectrum of the quantum clock model at various values of $\mu = h^{15/28}L$ in the two charge-conjugation sectors at $L = 64$.

$L = 64, \mu = 10.0, C = +$				
i	E_i^+	δE_i^+	j	n
0	-1.568088e+02	2.39e-04	0	0
1	-1.561719e+02	5.89e-04	1	0
2	-1.561228e+02	5.87e-04	1	1
3	-1.561228e+02	4.57e-04	1	1

$L = 64, \mu = 10.0, C = -$				
i	E_i^-	δE_i^-	j	n
0	-1.558925e+02	2.18e-03	1	0
1	-1.558575e+02	1.85e-03	1	1
2	-1.558575e+02	1.68e-03	1	1
3	-1.557604e+02	2.18e-03	1	2

$L = 64, \mu = 12.0, C = +$				
i	E_i^+	δE_i^+	j	n
0	-1.572059e+02	1.25e-04	0	0
1	-1.564413e+02	3.67e-04	1	0
2	-1.564000e+02	3.69e-04	1	1
3	-1.564000e+02	3.01e-04	1	1

$L = 64, \mu = 12.0, C = -$				
i	E_i^-	δE_i^-	j	n
0	-1.561090e+02	1.06e-03	1	0
1	-1.560799e+02	9.92e-04	1	1
2	-1.560799e+02	9.29e-04	1	1
3	-1.559969e+02	1.29e-03	1	2

$L = 64, \mu = 14.0, C = +$				
i	E_i^+	δE_i^+	j	n
0	-1.576747e+02	1.24e-04	0	0
1	-1.567820e+02	5.15e-03	1	0
2	-1.567467e+02	4.87e-03	1	1
3	-1.567468e+02	7.58e-03	1	1
4	-1.566478e+02	1.41e-03	1	2
5	-1.566478e+02	9.51e-03	1	2

$L = 64, \mu = 14.0, C = -$				
i	E_i^-	δE_i^-	j	n
0	-1.563982e+02	7.24e-04	1	0
1	-1.563732e+02	6.01e-04	1	1
2	-1.563732e+02	6.14e-04	1	1
3	-1.563009e+02	8.28e-04	1	2
4	-1.563009e+02	8.15e-04	1	2
5	-1.561885e+02	1.14e-03	1	3

TABLE S8. Low energy spectrum of the quantum clock model at various values of $\mu = h^{15/28}L$ in the two charge-conjugation sectors at $L = 64$.

$L = 80, \mu = 0.0, C = +$				
i	E_i^+	δE_i^+	j	n
0	-1.948929e+02	2.99e-03	0	0
1	-1.948656e+02	2.50e-03	1	0
2	-1.946615e+02	4.71e-03	1	1
3	-1.947282e+02	6.46e-03	2	0

$L = 80, \mu = 0.0, C = -$				
i	E_i^-	δE_i^-	j	n
0	-1.948656e+02	1.41e-03	1	0
1	-1.946615e+02	5.52e-03	1	1
2	-1.946615e+02	4.46e-03	1	1
3	-1.946209e+02	7.85e-03	2	0

$L = 80, \mu = 0.5, C = +$				
i	E_i^+	δE_i^+	j	n
0	-1.948930e+02	2.98e-03	0	0
1	-1.948668e+02	2.58e-03	1	0
2	-1.946621e+02	5.50e-03	1	1
3	-1.947282e+02	6.47e-03	2	0

$L = 80, \mu = 0.5, C = -$				
i	E_i^-	δE_i^-	j	n
0	-1.948644e+02	1.42e-03	1	0
1	-1.946608e+02	5.36e-03	1	1
2	-1.946608e+02	4.81e-03	1	1
3	-1.946210e+02	7.85e-03	2	0

$L = 80, \mu = 0.75, C = +$				
i	E_i^+	δE_i^+	j	n
0	-1.948934e+02	2.88e-03	0	0
1	-1.948679e+02	2.73e-03	1	0

$L = 80, \mu = 0.75, C = -$				
i	E_i^-	δE_i^-	j	n
0	-1.948630e+02	1.80e-03	1	0
1	-1.946601e+02	5.56e-03	1	1

$L = 80, \mu = 1.0, C = +$				
i	E_i^+	δE_i^+	j	n
0	-1.948943e+02	2.78e-03	0	0
1	-1.948688e+02	2.76e-03	1	0
2	-1.946640e+02	5.49e-03	1	1
3	-1.946640e+02	4.53e-03	1	1

$L = 80, \mu = 1.0, C = -$				
i	E_i^-	δE_i^-	j	n
0	-1.948611e+02	1.44e-03	1	0
1	-1.946591e+02	5.53e-03	1	1
2	-1.946591e+02	4.77e-03	1	1
3	-1.946211e+02	7.85e-03	2	0

$L = 80, \mu = 2.0, C = +$				
i	E_i^+	δE_i^+	j	n
0	-1.949101e+02	1.69e-03	0	0
1	-1.948661e+02	2.70e-03	1	0
2	-1.946712e+02	5.18e-03	1	1
3	-1.946712e+02	4.34e-03	1	1

$L = 80, \mu = 2.0, C = -$				
i	E_i^-	δE_i^-	j	n
0	-1.948492e+02	1.53e-03	1	0
1	-1.946534e+02	4.74e-03	1	1
2	-1.946534e+02	5.94e-03	1	1
3	-1.946220e+02	7.84e-03	2	0

$L = 80, \mu = 3.0, C = +$				
i	E_i^+	δE_i^+	j	n
0	-1.949451e+02	9.21e-04	0	0
1	-1.948537e+02	2.88e-03	1	0
2	-1.946840e+02	4.63e-03	1	1
3	-1.946840e+02	4.13e-03	1	1

$L = 80, \mu = 3.0, C = -$				
i	E_i^-	δE_i^-	j	n
0	-1.948309e+02	1.70e-03	1	0
1	-1.946463e+02	6.36e-03	1	1
2	-1.946463e+02	5.11e-03	1	1
3	-1.946248e+02	7.82e-03	2	0

TABLE S9. Low energy spectrum of the quantum clock model at various values of $\mu = h^{15/28}L$ in the two charge-conjugation sectors at $L = 80$.

$L = 80, \mu = 4.0, C = +$				
i	E_i^+	δE_i^+	j	n
0	-1.949957e+02	5.27e-04	0	0
1	-1.948383e+02	3.26e-03	1	0
2	-1.947042e+02	4.23e-03	1	1
3	-1.947042e+02	3.28e-03	1	1

$L = 80, \mu = 5.0, C = -$				
i	E_i^-	δE_i^-	j	n
0	-1.947795e+02	2.62e-03	1	0
1	-1.946420e+02	7.13e-03	1	1

$L = 80, \mu = 7.0, C = +$				
i	E_i^+	δE_i^+	j	n
0	-1.952350e+02	1.52e-04	0	0
1	-1.948807e+02	2.53e-03	1	0

$L = 80, \mu = 8.0, C = -$				
i	E_i^-	δE_i^-	j	n
0	-1.947582e+02	4.22e-03	1	0
1	-1.947201e+02	4.43e-03	1	1
2	-1.947201e+02	4.33e-03	1	1
3	-1.946426e+02	7.47e-03	2	0

$L = 80, \mu = 12.0, C = +$				
i	E_i^+	δE_i^+	j	n
0	-1.959225e+02	1.50e-04	0	0
1	-1.953111e+02	7.87e-04	1	0
2	-1.952780e+02	8.22e-04	1	1
3	-1.952780e+02	6.55e-04	1	1

$L = 80, \mu = 4.0, C = -$				
i	E_i^-	δE_i^-	j	n
0	-1.948072e+02	1.95e-03	1	0
1	-1.946410e+02	6.46e-03	1	1
2	-1.946410e+02	5.89e-03	1	1
3	-1.946306e+02	7.75e-03	2	0

$L = 80, \mu = 6.0, C = +$				
i	E_i^+	δE_i^+	j	n
0	-1.951407e+02	2.08e-04	0	0
1	-1.948427e+02	3.23e-03	1	0
2	-1.947729e+02	2.43e-03	1	1
3	-1.947729e+02	3.06e-03	1	1

$L = 80, \mu = 7.0, C = -$				
i	E_i^-	δE_i^-	j	n
0	-1.947374e+02	4.73e-03	1	0
1	-1.946804e+02	5.66e-03	1	1

$L = 80, \mu = 10.0, C = +$				
i	E_i^+	δE_i^+	j	n
0	-1.956043e+02	1.45e-04	0	0
1	-1.950950e+02	1.22e-03	1	0
2	-1.950557e+02	1.31e-03	1	1
3	-1.950557e+02	9.78e-04	1	1
4	-1.949521e+02	1.62e-03	1	2
5	-1.949521e+02	1.60e-03	1	2
6	-1.948090e+02	7.72e-03	1	3
7	-1.948082e+02	1.84e-02	1	3

$L = 80, \mu = 12.0, C = -$				
i	E_i^-	δE_i^-	j	n
0	-1.950421e+02	2.14e-03	1	0
1	-1.950188e+02	1.91e-03	1	1
2	-1.950188e+02	1.94e-03	1	1
3	-1.949525e+02	2.60e-03	1	2

$L = 80, \mu = 14.0, C = -$				
i	E_i^-	δE_i^-	j	n
0	-1.952731e+02	2.59e-03	1	0
1	-1.952532e+02	2.16e-03	1	1
2	-1.952532e+02	1.58e-03	1	1
3	-1.951953e+02	1.71e-03	1	2

$L = 80, \mu = 5.0, C = +$				
i	E_i^+	δE_i^+	j	n
0	-1.950609e+02	3.17e-04	0	0
1	-1.948294e+02	3.72e-03	1	0

$L = 80, \mu = 6.0, C = -$				
i	E_i^-	δE_i^-	j	n
0	-1.947516e+02	3.31e-03	1	0
1	-1.946544e+02	7.17e-03	1	1
2	-1.946544e+02	6.60e-03	1	1
3	-1.946544e+02	5.41e-03	2	0

$L = 80, \mu = 8.0, C = +$				
i	E_i^+	δE_i^+	j	n
0	-1.953437e+02	1.72e-04	0	0
1	-1.949370e+02	1.91e-03	1	0
2	-1.948881e+02	1.75e-03	1	1
3	-1.948881e+02	1.71e-03	1	1

$L = 80, \mu = 10.0, C = -$				
i	E_i^-	δE_i^-	j	n
0	-1.948692e+02	3.09e-03	1	0
1	-1.948413e+02	2.77e-03	1	1
2	-1.948413e+02	3.05e-03	1	1
3	-1.947637e+02	4.12e-03	1	2
4	-1.947637e+02	4.19e-03	1	2
5	-1.946484e+02	5.22e-03	1	3
6	-1.946484e+02	5.32e-03	1	3
7	-1.946274e+02	1.15e-02	2	0

$L = 80, \mu = 14.0, C = +$				
i	E_i^+	δE_i^+	j	n
0	-1.962981e+02	1.43e-04	0	0
1	-1.955845e+02	4.08e-03	1	0
2	-1.955559e+02	1.77e-02	1	1
3	-1.955560e+02	2.02e-03	1	1

TABLE S10. Low energy spectrum of the quantum clock model at various values of $\mu = h^{15/28}L$ in the two charge-conjugation sectors at $L = 80$.

$L = 96, \mu = 0.0, C = +$				
i	E_i^+	δE_i^+	j	n
0	-2.338665e+02	4.79e-03	0	0
1	-2.338438e+02	4.20e-03	1	0
2	-2.336736e+02	8.54e-03	1	1
3	-2.337294e+02	9.93e-03	2	0

$L = 96, \mu = 0.0, C = -$				
i	E_i^-	δE_i^-	j	n
0	-2.338438e+02	2.22e-03	1	0
1	-2.336736e+02	6.87e-03	1	1
2	-2.336736e+02	8.38e-03	1	1
3	-2.336398e+02	1.19e-02	2	0

$L = 96, \mu = 0.5, C = +$				
i	E_i^+	δE_i^+	j	n
0	-2.338666e+02	4.76e-03	0	0
1	-2.338447e+02	4.21e-03	1	0
2	-2.336742e+02	7.19e-03	1	1
3	-2.337294e+02	9.93e-03	2	0

$L = 96, \mu = 0.5, C = -$				
i	E_i^-	δE_i^-	j	n
0	-2.338427e+02	2.77e-03	1	0
1	-2.336731e+02	7.10e-03	1	1
2	-2.336731e+02	8.28e-03	1	1
3	-2.336398e+02	1.19e-02	2	0

$L = 96, \mu = 1.0, C = +$				
i	E_i^+	δE_i^+	j	n
0	-2.338677e+02	4.46e-03	0	0
1	-2.338464e+02	4.43e-03	1	0
2	-2.336757e+02	7.60e-03	1	1
3	-2.337295e+02	9.92e-03	2	0

$L = 96, \mu = 1.0, C = -$				
i	E_i^-	δE_i^-	j	n
0	-2.338400e+02	2.53e-03	1	0
1	-2.336717e+02	7.30e-03	1	1
2	-2.336717e+02	8.35e-03	1	1
3	-2.336400e+02	1.19e-02	2	0

$L = 96, \mu = 2.0, C = +$				
i	E_i^+	δE_i^+	j	n
0	-2.338808e+02	2.73e-03	0	0
1	-2.338442e+02	4.70e-03	1	0
2	-2.336817e+02	7.16e-03	1	1
3	-2.337303e+02	9.82e-03	2	0

$L = 96, \mu = 2.0, C = -$				
i	E_i^-	δE_i^-	j	n
0	-2.338301e+02	2.97e-03	1	0
1	-2.336669e+02	7.34e-03	1	1
2	-2.336669e+02	8.94e-03	1	1
3	-2.336407e+02	1.19e-02	2	0

$L = 96, \mu = 3.0, C = +$				
i	E_i^+	δE_i^+	j	n
0	-2.339100e+02	1.50e-03	0	0
1	-2.338338e+02	4.48e-03	1	0
2	-2.336925e+02	7.23e-03	1	1
3	-2.336925e+02	6.24e-03	1	1

$L = 96, \mu = 3.0, C = -$				
i	E_i^-	δE_i^-	j	n
0	-2.338148e+02	2.91e-03	1	0
1	-2.336609e+02	8.85e-03	1	1
2	-2.336609e+02	8.78e-03	1	1
3	-2.336429e+02	1.18e-02	2	0

$L = 96, \mu = 4.0, C = +$				
i	E_i^+	δE_i^+	j	n
0	-2.339522e+02	8.67e-04	0	0
1	-2.338210e+02	5.11e-03	1	0
2	-2.337093e+02	5.20e-03	1	1
3	-2.337395e+02	8.89e-03	2	0

$L = 96, \mu = 4.0, C = -$				
i	E_i^-	δE_i^-	j	n
0	-2.337951e+02	3.06e-03	1	0
1	-2.336565e+02	1.09e-02	1	1
2	-2.336565e+02	8.35e-03	1	1
3	-2.336477e+02	1.20e-02	2	0

$L = 96, \mu = 5.0, C = +$				
i	E_i^+	δE_i^+	j	n
0	-2.340066e+02	5.40e-04	0	0
1	-2.338136e+02	5.99e-03	1	0

$L = 96, \mu = 5.0, C = -$				
i	E_i^-	δE_i^-	j	n
0	-2.337720e+02	4.52e-03	1	0
1	-2.336573e+02	1.03e-02	1	1

$L = 96, \mu = 6.0, C = +$				
i	E_i^+	δE_i^+	j	n
0	-2.340731e+02	3.45e-04	0	0
1	-2.338248e+02	5.20e-03	1	0
2	-2.337666e+02	4.72e-03	1	1
3	-2.337666e+02	3.69e-03	1	1

$L = 96, \mu = 6.0, C = -$				
i	E_i^-	δE_i^-	j	n
0	-2.337487e+02	5.42e-03	1	0
1	-2.336675e+02	1.04e-02	1	1
2	-2.336675e+02	9.92e-03	1	1

$L = 96, \mu = 7.0, C = +$				
i	E_i^+	δE_i^+	j	n
0	-2.341517e+02	2.80e-04	0	0
1	-2.338566e+02	4.22e-03	1	0

$L = 96, \mu = 7.0, C = -$				
i	E_i^-	δE_i^-	j	n
0	-2.337366e+02	7.29e-03	1	0
1	-2.336890e+02	7.31e-03	1	1

TABLE S11. Low energy spectrum of the quantum clock model at various values of $\mu = h^{15/28} L$ in the two charge-conjugation sectors at $L = 96$.

$L = 96, \mu = 8.0, C = +$				
i	E_i^+	δE_i^+	j	n
0	-2.342424e+02	2.23e-04	0	0
1	-2.339035e+02	3.13e-03	1	0
2	-2.338628e+02	3.14e-03	1	1
3	-2.338628e+02	2.44e-03	1	1

$L = 96, \mu = 8.0, C = -$				
i	E_i^-	δE_i^-	j	n
0	-2.337538e+02	6.63e-03	1	0
1	-2.337220e+02	6.81e-03	1	1
2	-2.337220e+02	6.69e-03	1	1
3	-2.336577e+02	1.13e-02	2	0

$L = 96, \mu = 10.0, C = +$				
i	E_i^+	δE_i^+	j	n
0	-2.344597e+02	1.65e-04	0	0
1	-2.340354e+02	8.59e-03	1	0
2	-2.340027e+02	4.99e-03	1	1
3	-2.340028e+02	7.94e-03	1	1

$L = 96, \mu = 10.0, C = -$				
i	E_i^-	δE_i^-	j	n
0	-2.338460e+02	4.93e-03	1	0
1	-2.338228e+02	4.95e-03	1	1
2	-2.338228e+02	4.54e-03	1	1
3	-2.337581e+02	6.63e-03	1	2

$L = 96, \mu = 12.0, C = +$				
i	E_i^+	δE_i^+	j	n
0	-2.347251e+02	1.18e-03	0	0
1	-2.342158e+02	5.65e-03	1	0
2	-2.341883e+02	3.27e-03	1	1
3	-2.341883e+02	2.82e-03	1	1

$L = 96, \mu = 12.0, C = -$				
i	E_i^-	δE_i^-	j	n
0	-2.339899e+02	4.15e-03	1	0
1	-2.339705e+02	3.41e-03	1	1
2	-2.339705e+02	3.41e-03	1	1
3	-2.339153e+02	4.62e-03	1	2

$L = 96, \mu = 14.0, C = +$				
i	E_i^+	δE_i^+	j	n
0	-2.350385e+02	1.70e-04	0	0
1	-2.344440e+02	7.04e-03	1	0
2	-2.344204e+02	6.04e-03	1	1
3	-2.344204e+02	4.54e-03	1	1

$L = 96, \mu = 14.0, C = -$				
i	E_i^-	δE_i^-	j	n
0	-2.341817e+02	1.60e-02	1	0
1	-2.341661e+02	1.37e-02	1	1
2	-2.341657e+02	4.88e-03	1	1
3	-2.341175e+02	4.90e-03	1	2

TABLE S12. Low energy spectrum of the quantum clock model at various values of $\mu = h^{15/28}L$ in the two charge-conjugation sectors at $L = 96$.

B. String tension data tables

$L = 24, \mu = 8.0$			$L = 24, \mu = 10.0$			$L = 24, \mu = 12.0$			$L = 24, \mu = 14.0$		
w	$V(w)$	$\delta V(w)$	w	$V(w)$	$\delta V(w)$	w	$V(w)$	$\delta V(w)$	w	$V(w)$	$\delta V(w)$
4	2.012132e-01	1.03e-04	4	3.128000e-01	3.22e-04	4	4.483738e-01	4.68e-04	4	6.077639e-01	5.80e-04
8	3.996440e-01	1.03e-04	8	6.214558e-01	3.22e-04	8	8.911704e-01	4.69e-04	8	1.208491e+00	5.79e-04
12	5.972413e-01	1.03e-04	12	9.291092e-01	3.22e-04	12	1.332845e+00	4.69e-04	12	1.808025e+00	5.79e-04
16	7.944358e-01	1.03e-04	16	1.236398e+00	3.22e-04	16	1.774182e+00	4.69e-04	16	2.407247e+00	5.79e-04
20	9.907450e-01	1.03e-04	20	1.543044e+00	3.22e-04	20	2.215048e+00	4.69e-04	20	3.006129e+00	5.79e-04
24	1.164693e+00	1.03e-04	24	1.827856e+00	3.28e-04	24	2.634603e+00	8.10e-04	24	3.584148e+00	1.07e-02

$L = 32, \mu = 8.0$			$L = 32, \mu = 10.0$			$L = 32, \mu = 12.0$			$L = 32, \mu = 14.0$		
w	$V(w)$	$\delta V(w)$	w	$V(w)$	$\delta V(w)$	w	$V(w)$	$\delta V(w)$	w	$V(w)$	$\delta V(w)$
4	1.138530e-01	1.34e-04	4	1.770976e-01	1.41e-04	4	2.539904e-01	6.47e-04	4	3.444423e-01	1.30e-03
8	2.261135e-01	1.34e-04	8	3.517286e-01	1.40e-04	8	5.045379e-01	6.47e-04	8	6.843963e-01	1.30e-03
12	3.377887e-01	1.35e-04	12	5.255936e-01	1.40e-04	12	7.541680e-01	6.47e-04	12	1.023315e+00	1.30e-03
16	4.491967e-01	1.34e-04	16	6.991571e-01	1.40e-04	16	1.003478e+00	6.47e-04	16	1.361908e+00	1.30e-03
20	5.604434e-01	1.34e-04	20	8.725754e-01	1.40e-04	20	1.252653e+00	6.47e-04	20	1.700378e+00	1.30e-03
24	6.714636e-01	1.34e-04	24	1.045838e+00	1.40e-04	24	1.501721e+00	6.47e-04	24	2.038771e+00	1.30e-03
28	7.816185e-01	1.34e-04	28	1.218395e+00	1.40e-04	28	1.750203e+00	6.47e-04	28	2.376693e+00	1.30e-03
32	8.760565e-01	1.36e-04	32	1.375504e+00	1.38e-03	32	1.983548e+00	7.43e-03	32	2.699641e+00	1.02e-02

$L = 48, \mu = 8.0$			$L = 48, \mu = 10.0$			$L = 48, \mu = 12.0$			$L = 48, \mu = 14.0$		
w	$V(w)$	$\delta V(w)$	w	$V(w)$	$\delta V(w)$	w	$V(w)$	$\delta V(w)$	w	$V(w)$	$\delta V(w)$
6	7.615200e-02	1.61e-04	6	1.185266e-01	1.82e-04	6	1.700922e-01	1.51e-04	6	2.307957e-01	3.26e-03
12	1.512154e-01	1.59e-04	12	2.353552e-01	1.82e-04	12	3.377931e-01	1.51e-04	12	4.584525e-01	3.26e-03
18	2.258822e-01	1.58e-04	18	3.516640e-01	1.83e-04	18	5.048706e-01	1.52e-04	18	6.854037e-01	3.26e-03
24	3.003691e-01	1.57e-04	24	4.677693e-01	1.82e-04	24	6.717320e-01	1.53e-04	24	9.121365e-01	3.26e-03
30	3.747475e-01	1.58e-04	30	5.837776e-01	1.82e-04	30	8.385046e-01	1.53e-04	30	1.138788e+00	3.26e-03
36	4.489742e-01	1.58e-04	36	6.996813e-01	1.80e-04	36	1.005204e+00	1.53e-04	36	1.365388e+00	3.26e-03
42	5.226211e-01	1.64e-04	42	8.151069e-01	1.80e-04	42	1.171504e+00	1.51e-04	42	1.591664e+00	3.26e-03
48	5.858712e-01	3.91e-04	48	9.203349e-01	9.49e-04	48	1.327782e+00	8.51e-04	48	1.807970e+00	3.26e-03

TABLE S13. Static quark-antiquark potential as a function of w at various L and μ .

$L = 64, \mu = 8.0$			$L = 64, \mu = 10.0$			$L = 64, \mu = 12.0$			$L = 64, \mu = 14.0$		
w	$V(w)$	$\delta V(w)$	w	$V(w)$	$\delta V(w)$	w	$V(w)$	$\delta V(w)$	w	$V(w)$	$\delta V(w)$
8	5.721387e-02	1.82e-04	8	8.907968e-02	2.71e-04	8	1.278724e-01	1.80e-04	8	1.735599e-01	1.78e-04
16	1.136023e-01	1.82e-04	16	1.768672e-01	2.69e-04	16	2.539211e-01	1.80e-04	16	3.447157e-01	1.79e-04
24	1.696913e-01	1.83e-04	24	2.642611e-01	2.68e-04	24	3.794974e-01	1.79e-04	24	5.153385e-01	1.77e-04
32	2.256446e-01	1.85e-04	32	3.515027e-01	2.68e-04	32	5.049111e-01	1.79e-04	32	6.857967e-01	1.79e-04
40	2.815159e-01	1.96e-04	40	4.386707e-01	2.69e-04	40	6.302583e-01	1.79e-04	40	8.561941e-01	1.80e-04
48	3.372727e-01	2.22e-04	48	5.257600e-01	2.70e-04	48	7.555511e-01	1.78e-04	48	1.026553e+00	1.79e-04
56	3.925950e-01	2.84e-04	56	6.124890e-01	2.86e-04	56	8.805406e-01	1.76e-04	56	1.196665e+00	1.77e-04
64	4.401559e-01	1.84e-03	64	6.916192e-01	2.50e-03	64	9.980791e-01	3.83e-03	64	1.359393e+00	4.68e-03

$L = 80, \mu = 8.0$			$L = 80, \mu = 10.0$			$L = 80, \mu = 12.0$			$L = 80, \mu = 14.0$		
w	$V(w)$	$\delta V(w)$	w	$V(w)$	$\delta V(w)$	w	$V(w)$	$\delta V(w)$	w	$V(w)$	$\delta V(w)$
8	3.673600e-02	2.22e-04	8	5.721413e-02	1.99e-04	8	8.215093e-02	2.08e-04	8	1.115261e-01	2.05e-04
16	7.295840e-02	2.27e-04	16	1.136037e-01	2.01e-04	16	1.631093e-01	2.06e-04	16	2.214477e-01	2.03e-04
24	1.089648e-01	2.33e-04	24	1.696941e-01	2.02e-04	24	2.436925e-01	2.03e-04	24	3.309269e-01	2.04e-04
32	1.448640e-01	2.48e-04	32	2.256525e-01	2.01e-04	32	3.241269e-01	2.03e-04	32	4.402469e-01	2.04e-04
40	1.807040e-01	2.68e-04	48	3.374045e-01	2.17e-04	40	4.044949e-01	2.03e-04	40	5.495013e-01	2.02e-04
48	2.165032e-01	2.99e-04	40	2.815469e-01	2.05e-04	48	4.848293e-01	2.11e-04	48	6.587261e-01	2.04e-04
56	2.522544e-01	3.44e-04	64	4.489725e-01	2.73e-04	56	5.651405e-01	2.13e-04	56	7.679333e-01	2.03e-04
64	2.878936e-01	4.18e-04	56	3.932293e-01	2.38e-04	64	6.453933e-01	2.24e-04	64	8.771005e-01	2.03e-04
72	3.231280e-01	1.28e-03	72	5.043525e-01	7.63e-04	72	7.253093e-01	2.63e-04	72	9.859621e-01	2.14e-04
80	3.525112e-01	2.17e-03	80	5.539981e-01	2.62e-03	80	7.997117e-01	6.92e-03	80	1.089283e+00	5.78e-03

$L = 96, \mu = 8.0$			$L = 96, \mu = 10.0$			$L = 96, \mu = 12.0$			$L = 96, \mu = 14.0$		
w	$V(w)$	$\delta V(w)$	w	$V(w)$	$\delta V(w)$	w	$V(w)$	$\delta V(w)$	w	$V(w)$	$\delta V(w)$
8	2.557248e-02	3.01e-04	8	3.983936e-02	2.26e-04	8	5.721472e-02	1.19e-03	8	7.768640e-02	2.34e-04
16	5.080320e-02	3.07e-04	16	7.911584e-02	2.26e-04	16	1.136032e-01	1.19e-03	16	1.542445e-01	2.35e-04
24	7.587264e-02	3.25e-04	24	1.181638e-01	2.28e-04	24	1.696941e-01	1.19e-03	24	2.304397e-01	2.27e-04
32	1.008576e-01	3.60e-04	32	1.571005e-01	2.36e-04	32	2.256525e-01	1.19e-03	32	3.064890e-01	2.27e-04
40	1.257926e-01	3.93e-04	40	1.959786e-01	2.55e-04	40	2.815475e-01	1.19e-03	40	3.824710e-01	2.34e-04
48	1.506960e-01	4.40e-04	48	2.348240e-01	2.77e-04	48	3.374099e-01	1.20e-03	48	4.584214e-01	2.37e-04
56	1.755763e-01	4.84e-04	56	2.736483e-01	3.18e-04	56	3.932522e-01	1.20e-03	56	5.343555e-01	2.37e-04
64	2.004307e-01	5.41e-04	64	3.124544e-01	3.49e-04	64	4.490819e-01	1.20e-03	64	6.102781e-01	2.42e-04
72	2.252429e-01	2.85e-03	72	3.512307e-01	3.93e-04	72	5.048915e-01	1.21e-03	72	6.861882e-01	2.49e-04
80	2.499408e-01	7.42e-04	80	3.899168e-01	4.73e-04	80	5.606291e-01	1.22e-03	80	7.620435e-01	2.65e-04
88	2.743171e-01	7.53e-03	88	4.285693e-01	1.47e-02	88	6.160298e-01	2.08e-03	88	8.375696e-01	4.22e-04
96	2.939818e-01	2.31e-03	96	4.620790e-01	3.20e-03	96	6.674579e-01	1.66e-02	96	9.088966e-01	9.01e-03

TABLE S14. Static quark-antiquark potential as a function of w at various L and μ .

C. Plots that determine $R(\mu)$ from the DMRG data

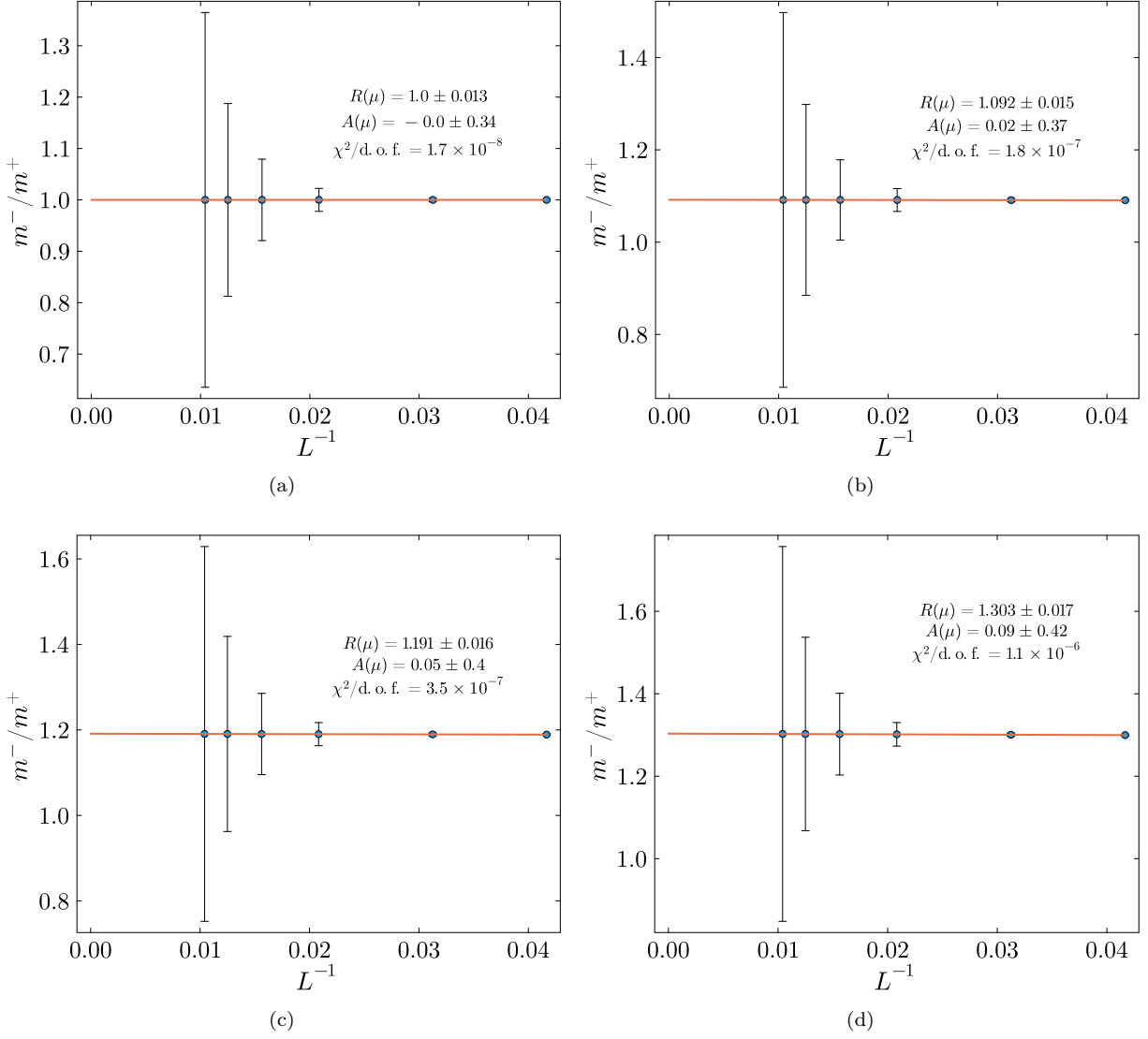


FIG. S1. Mass ratio scaling at (a) $\mu = 0.0$, (b) $\mu = 0.5$, (c) $\mu = 0.75$, (d) $\mu = 1.0$. The lowest glueball masses in the charge-conjugation-even and -odd sectors are given by the expression $m^\pm = E_1^\pm - E_0^+$, using the values given in Section A.

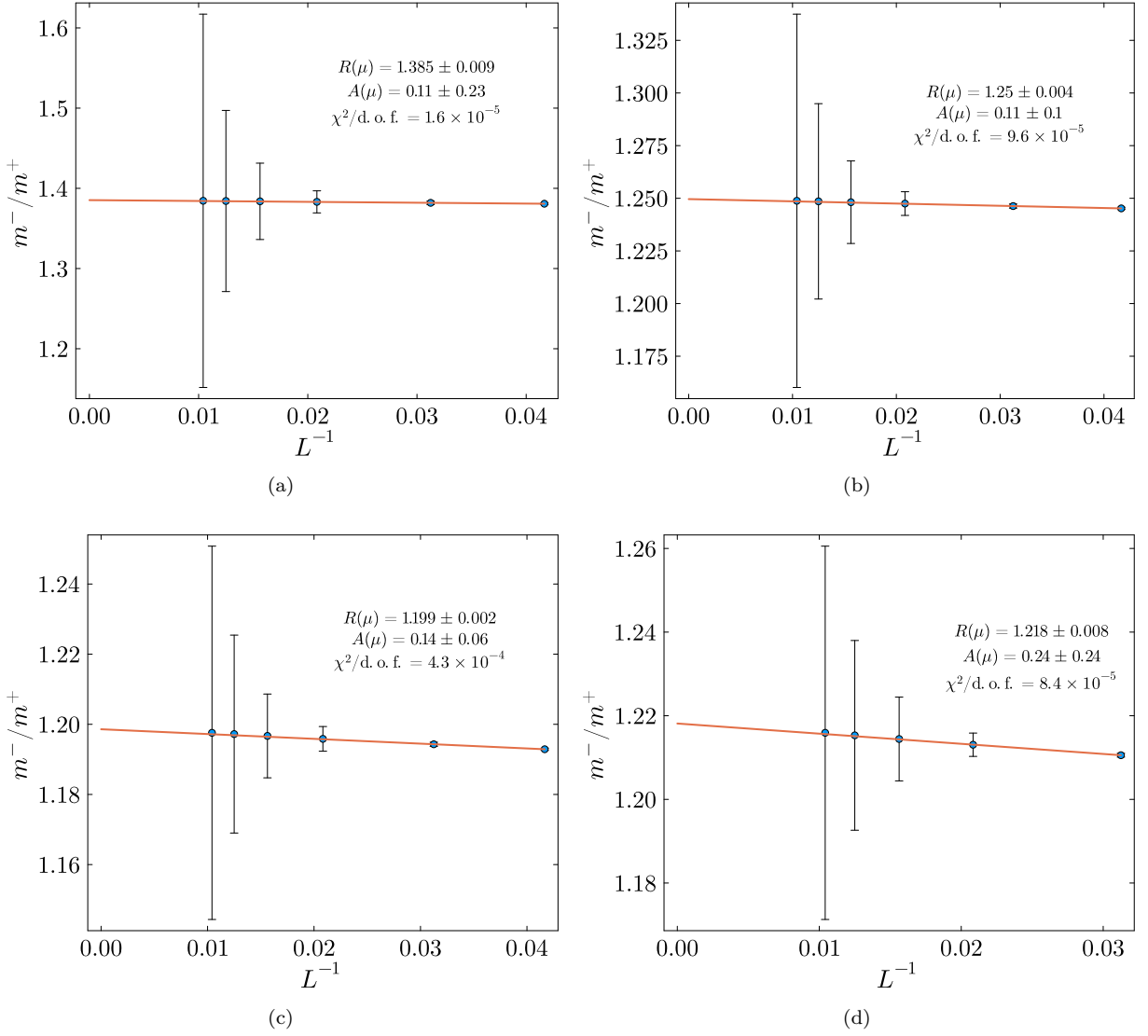


FIG. S2. Mass ratio scaling at (a) $\mu = 2.0$, (b) $\mu = 3.0$, (c) $\mu = 4.0$, (d) $\mu = 5.0$. The lowest glueball masses in the charge-conjugation-even and -odd sectors are given by the expression $m^\pm = E_1^\pm - E_0^+$, using the values given in Section A.

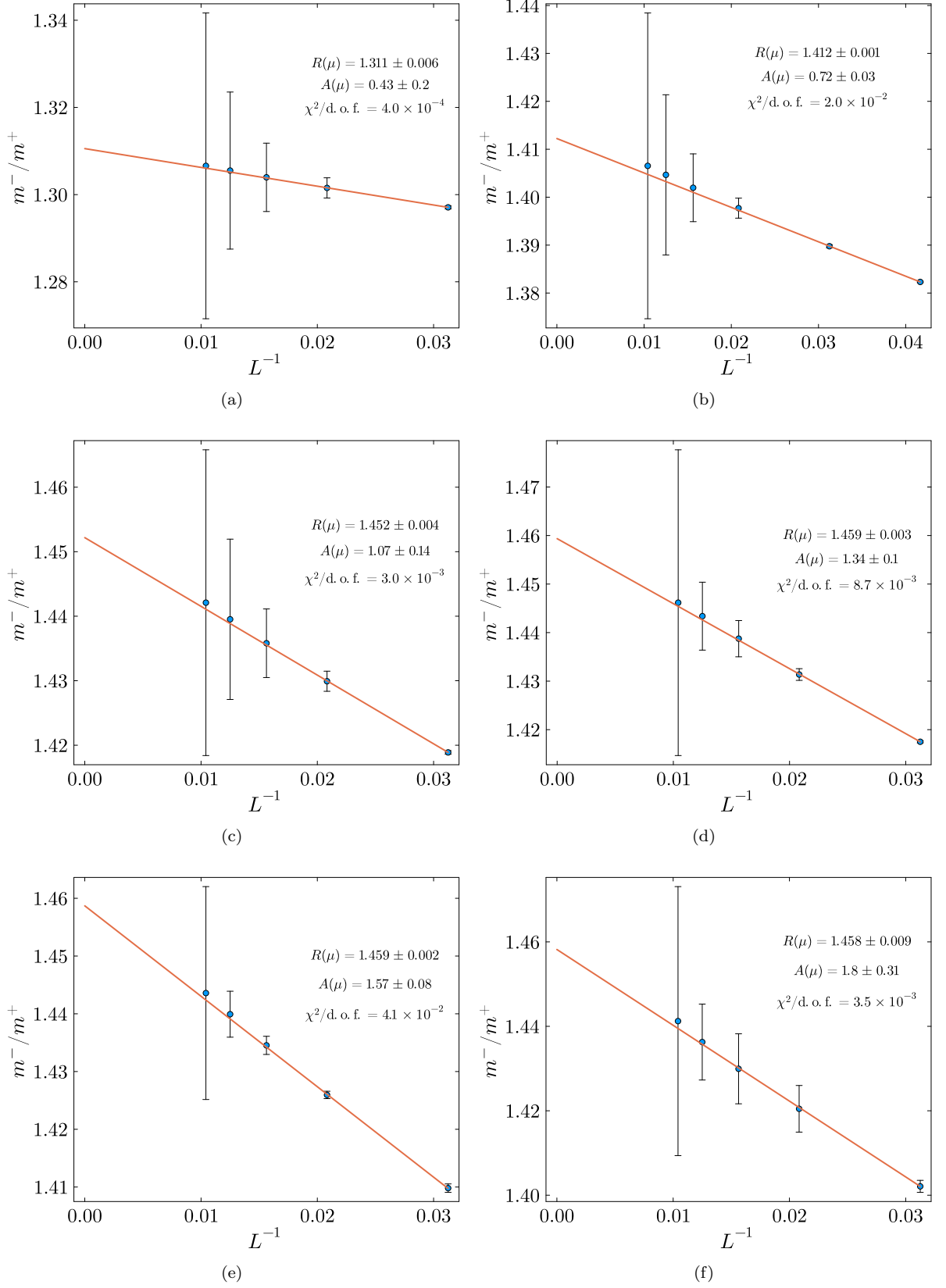
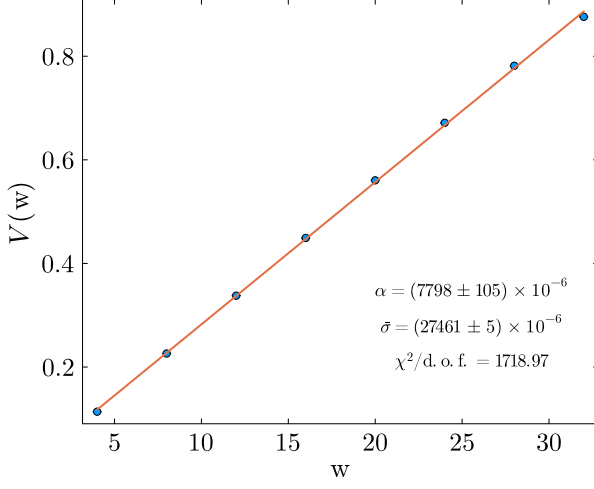
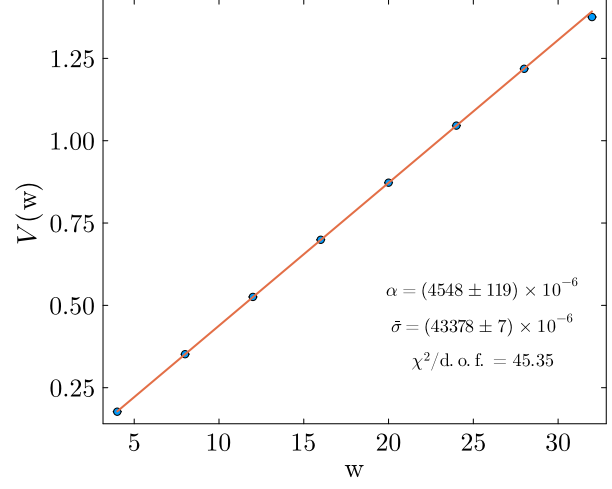


FIG. S3. Mass ratio scaling at (a) $\mu = 6.0$, (b) $\mu = 7.0$, (c) $\mu = 8.0$, (d) $\mu = 10.0$, (e) $\mu = 12.0$, (f) $\mu = 14.0$. The lowest glueball masses in the charge-conjugation-even and -odd sectors are given by the expression $m^\pm = E_1^\pm - E_0^+$, using the values given in Section A.

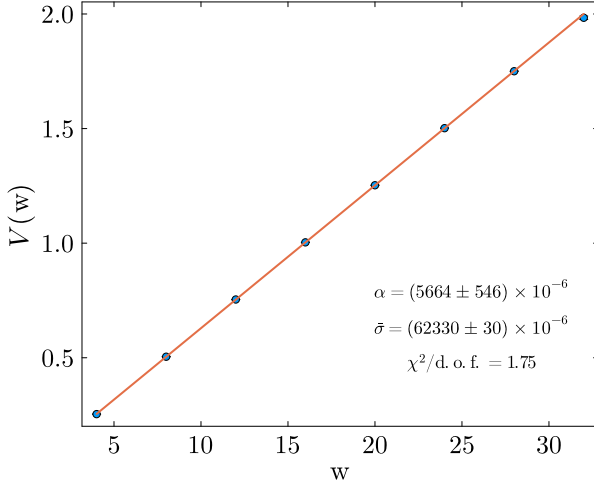
D. Plots that determine $\bar{\sigma}$ from the DMRG data



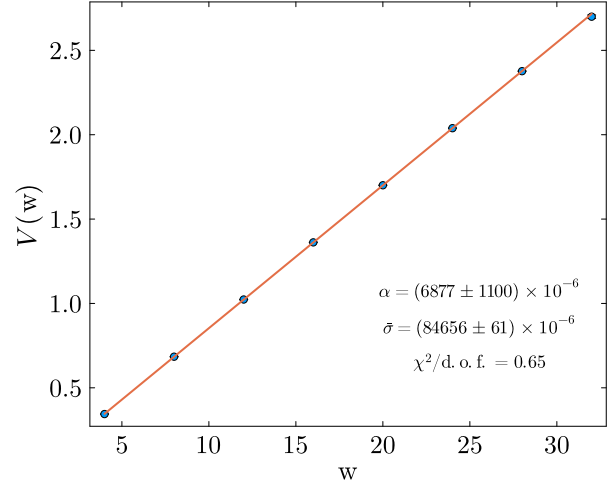
(a)



(b)



(c)



(d)

FIG. S4. Static quark potential $V(w)$ versus separation w for $L = 32$ at (a) $\mu = 8.0$, (b) $\mu = 10.0$, (c) $\mu = 12.0$, (d) $\mu = 14.0$.

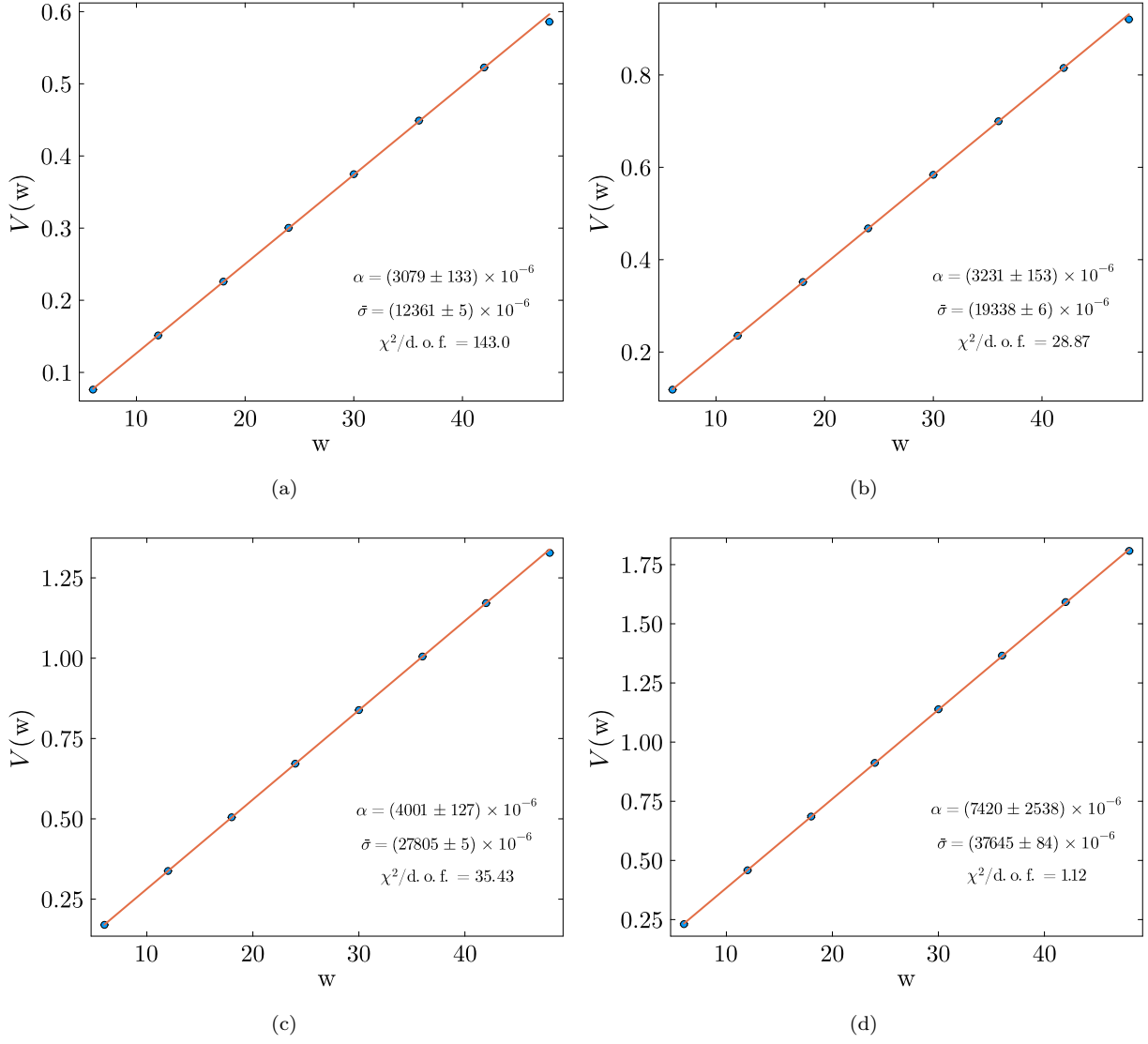


FIG. S5. Static quark potential $V(w)$ versus separation w for $L = 48$ at (a) $\mu = 8.0$, (b) $\mu = 10.0$, (c) $\mu = 12.0$, (d) $\mu = 14.0$.

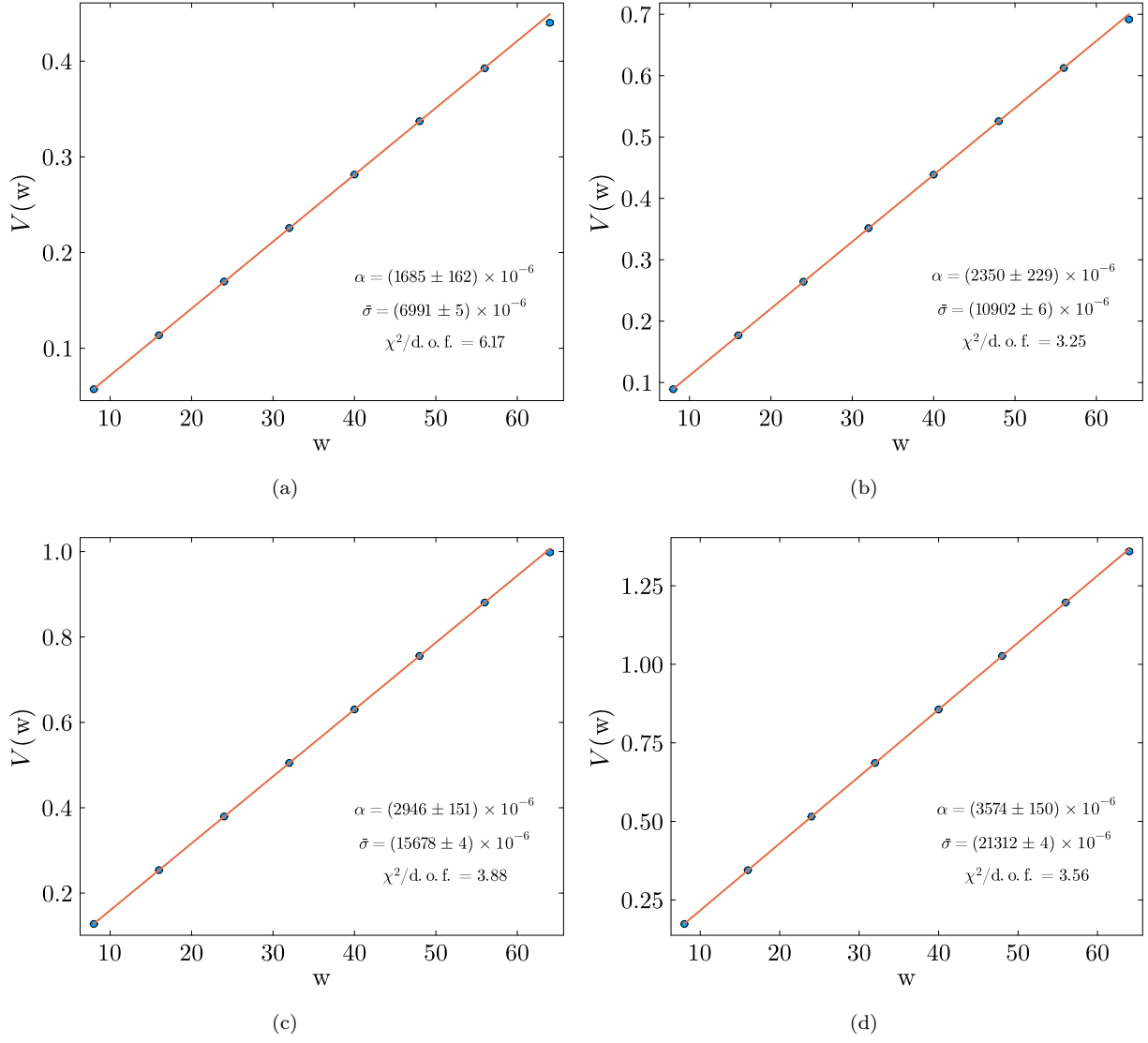


FIG. S6. Static quark potential $V(w)$ versus separation w for $L = 64$ at (a) $\mu = 8.0$, (b) $\mu = 10.0$, (c) $\mu = 12.0$, (d) $\mu = 14.0$.

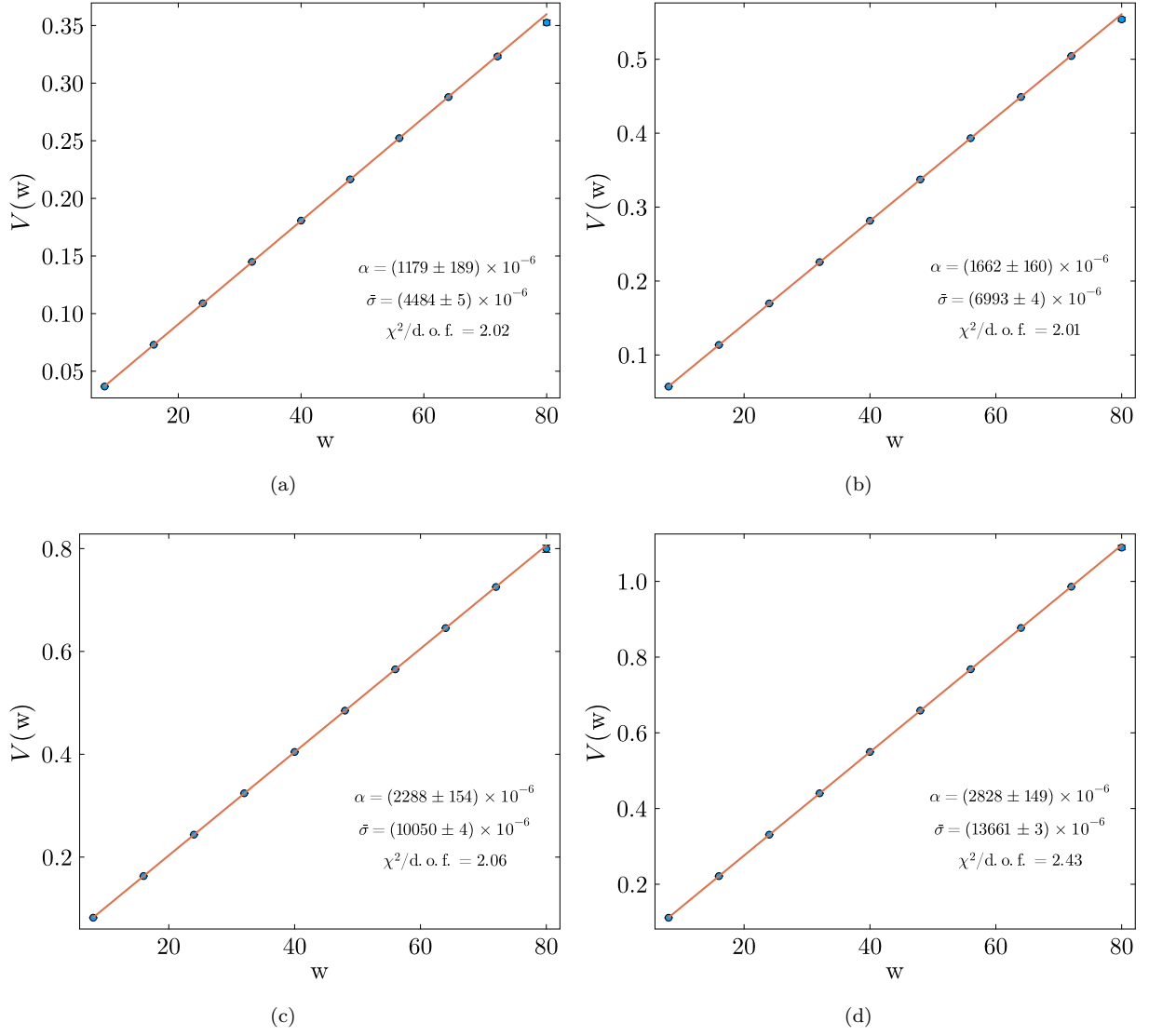
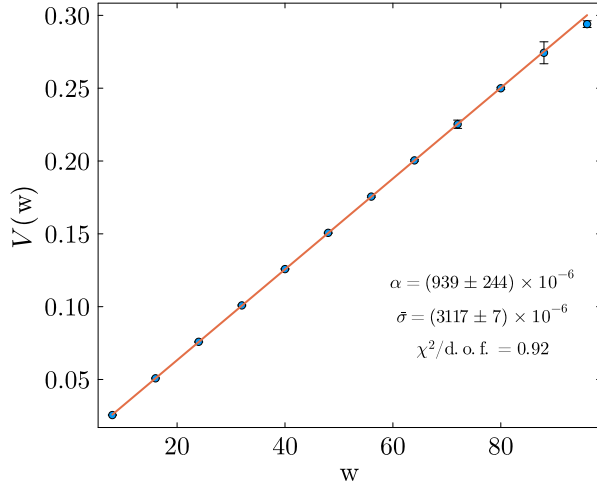
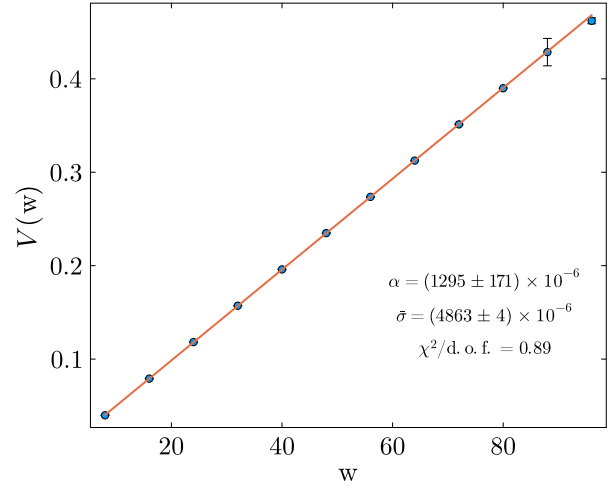


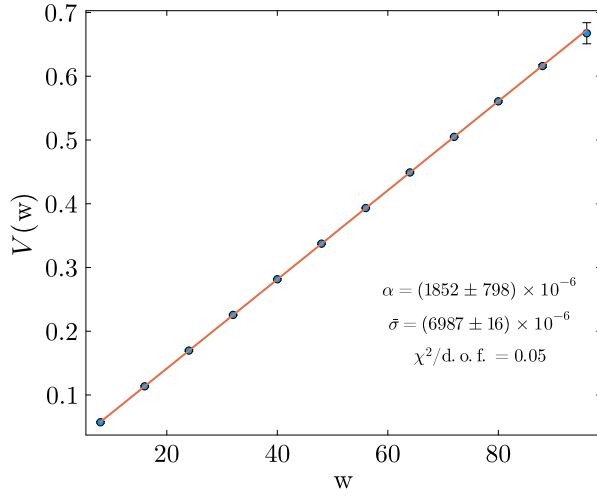
FIG. S7. Static quark potential $V(w)$ versus separation w for $L = 80$ at (a) $\mu = 8.0$, (b) $\mu = 10.0$, (c) $\mu = 12.0$, (d) $\mu = 14.0$.



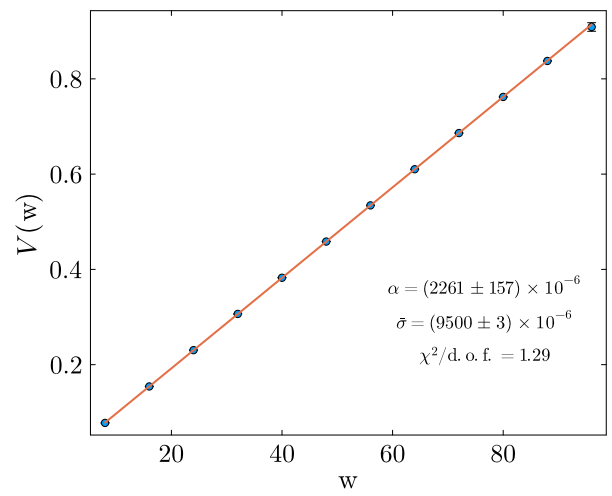
(a)



(b)



(c)



(d)

FIG. S8. Static quark potential $V(w)$ versus separation w for $L = 96$ at (a) $\mu = 8.0$, (b) $\mu = 10.0$, (c) $\mu = 12.0$, (d) $\mu = 14.0$.

E. Plots that determine $\sqrt{\bar{\sigma}}/m^+$

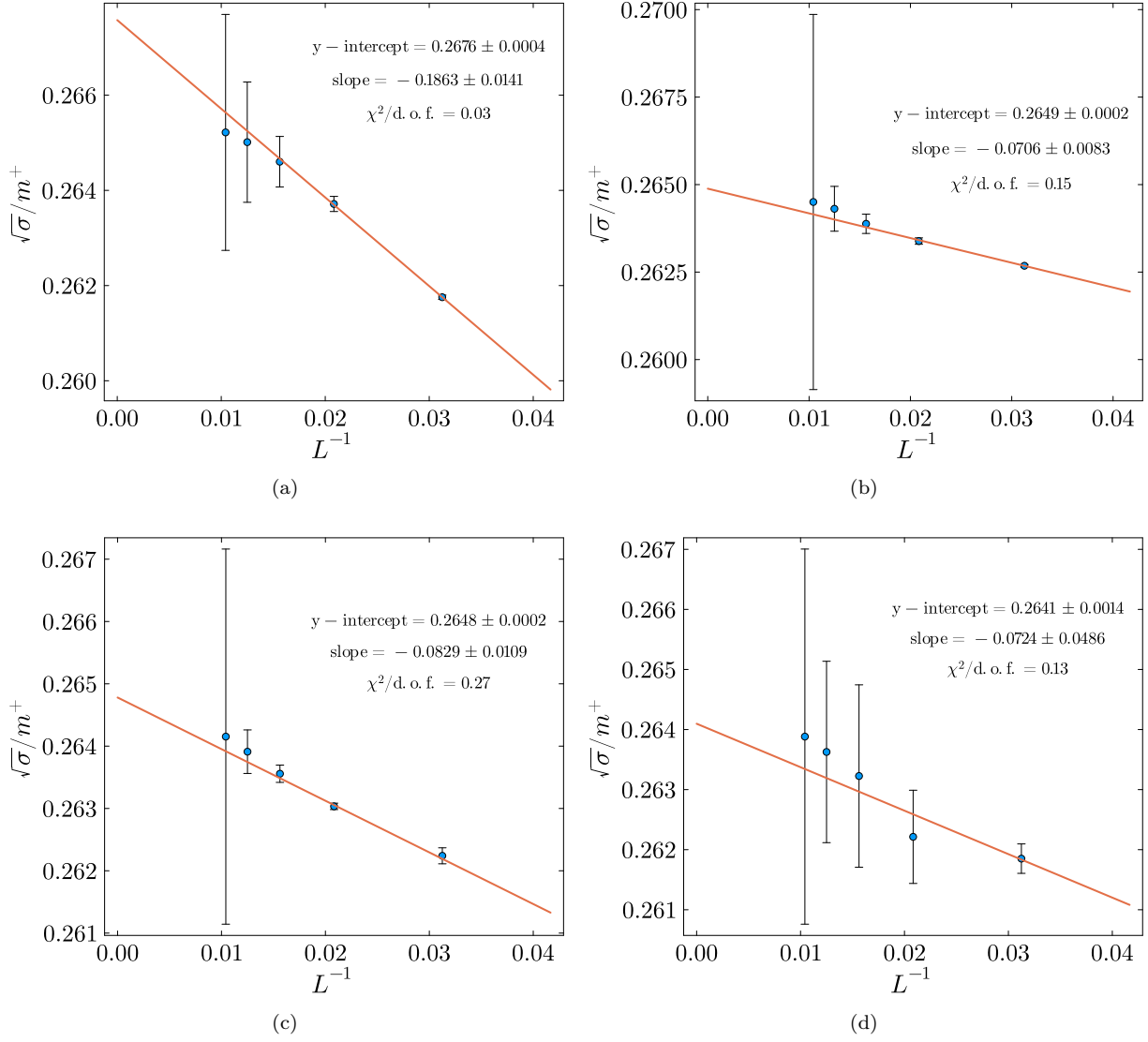


FIG. S9. String tension scaling at (a) $\mu = 8.0$, (b) $\mu = 10.0$, (c) $\mu = 12.0$, (d) $\mu = 14.0$. Each data point is computed using $\zeta = 2.5907(2)$, values of $\bar{\sigma}$ obtained in Section D, the definition $\sigma = \bar{\sigma}\zeta$, and the values of $m^+ = E_1^+ - E_0^+$ from Section A.